REMARKS

Claims 31-33 and 48-50 have been amended to remove dependencies on non-elected claims, by incorporating language from the non-elected claims. The Specification has been amended to correct typographical errors. No new matter has been added.

Restriction Requirement

Applicant appreciates the Examiner's reconsideration of the restriction requirement and withdrawal of the species election requirement.

Specification

The Examiner objected to the Specification as not complying with 1.821(d) of the sequence rules. The Specification has been amended to comply with §1.821(d) of the Sequence Rules and Regulations. Applicant notes that the sequence RRKRK is SEQ ID NO: 10, and that a typographical error in one sequence (p. 33, line 22, sequence "RRKESS") has been corrected ("RRKRKESS"). This amendment finds support in the text itself on p. 33, which indicates that a peptide with three residues following the RRKRK motif was an antagonist.

Rejection of Claims under 35 U.S.C. 112, second paragraph

The Examiner rejected Claims 31-33 and 48-50, stating that the claims were drawn to non-elected inventions of Claims 16, 19 and 20. The claims have been amended to remove the dependency on the non-elected claims.

Rejection of Claims under 35 U.S.C. 102

Claim 31

The Examiner rejected Claim 31 under 35 U.S.C. 102(b), as being anticipated by Ohashi *et al.* (*Biochem. Biophys. Res. Commun.* 195: 1314-1320(1993)), stating that Osashi *et al.* disclose a method of activating eNOS by contacting eNOS with phospholipids, and that it is reasonable to assume the phospholipids activated eNOS by antagonizing the autoinhibition of amino acids 590-650 of eNOS.

Ohashi *et al.* describe the effects of the phospholipids phosphatidylcholine, lysophasphatidylcholine, and phosphatidylethanolamine on nitric oxide synthase. They indicate that the phospholipids enhanced enzyme activity in the presence of Ca2, calmodulin, NADPH, FAD, and (6R)-5,6,7,8-tetrahydrobiopterin, in an additive manner.

The additive enhancement of activity of eNOS by the phospholipids does not *per se* indicate that the phospholipids activate eNOS by antagonizing autoinhibition of amino acids 590-650 of eNOS. In fact, the data provided by Ohashi *et al.* appear to be contrary to antagonizing autoinhibition of amino acids 590-650 of eNOS. As described in detail in the Specification, amino acids 590-650 serve as a control site for eNOS. Control site activator effects generally are not additive to the effect of activation with calcium/calmodulin, but instead produce activation at lower levels of calcium/calmodulin (see, e.g., Salerno, J.C. et al., *J. Biol. Chem. 272*:29769-29777 (1997), a copy of which is attached as Exhibit A for the convenience of the Examiner). Furthermore, the phospholipid effects are most likely due to solubility and aggregations issues, as all purified NOS mammalian isoforms require glycerol to retain solubility and full activity (see, e.g., Roman, L.J. et al., PNAS (USA) 92(18):8428-8432 (1995), a copy of which is attached as Exhibit B for the convenience of the Examiner). This is further supported by discussion on p. 1319 of Ohashi *et al.*, which indicates that micelle formation may provide a hydrophobic milieu stabilizing and maintaining the enzyme in an active conformation.

In view of these considerations, Claim 31 is not anticipated by the teachings of Ohashi *et al.*

Claim 33

The Examiner rejected Claim 33 under 35 U.S.C. 102(b), as being anticipated by either Hu *et al.* (*NeuroReport* 1993: 4:760-762) or Hashida-Okumura *et al.* (*J. Clin. Biochem. Nutrit.* 1994: 17:141-151), stating that Hu *et al.* teach activating neuronal NOS by contacting nNOS with the B-amyloid peptide, amino acids 25-35, and that Hashida-Okumura *et al.* teach a method of activating brain NOS by contacting the NOS with a partially purified factor isolated from urine.

Hu *et al.* describe experiments in which mouse neuroblastoma N1E-115 cells were exposed to β-amyloid 25-35, resulting in generation and release of nitric oxide. Activation of

NOS was assessed by measuring the release of nitric oxide, which was identified by an increase in cyclic GMP formation. Additional experiments indicated that the reaction was due to dependence on calcium ion influx into the cells (see p. 762, first paragraph).

Hu *et al.* do not describe contacting the neuronal nitric oxide synthase with an activator of neuronal nitric oxide synthase. There is no contact between the neuronal NOS and the β-amyloid 25-35, as all of the reactions described by Hu *et al.* take place in a cell-based system. The β-amyloid 25-35 was added to the culture medium of the cells (see Fig. 1). Furthermore, a nitric oxide scavenger (hemoglobin) attenuated the formation of cyclic GMP formation by β-amyloid 25-35; hemoglobin does not penetrate the cell membrane (see p. 762, second paragraph). Akama *et al.* (PNAS 95(10):5795-800 (1998), a copy of which is attached to this Amendment as Exhibit C), state that an NFκB-dependent mechanism is involved in reactions such as those described by Hu *et al.*, and indicate that it is pathway-dependent (in contrast to the direct result of contact between the agent and the NOS as set forth in the claims).

In view of these considerations, Claim 33 is not anticipated by the teachings of Hu *et al.*

Hashida-Okumura *et al.* describe a factor purified from rat urine that activates brain NOS. Activation of NOS was assessed by measuring the release of nitric oxide, which was identified by the formation of breakdown products of NO. Hashida-Okomura *et al.* indicate that the factor is very similar to the cofactor flavin adenine dinucleotide (FAD) (see p. 150). In fact, a later publication by the same group explores the effects of FAD on NOS; the further research was conducted because of the results obtained by Hashida-Okumura *et al.* (see, e.g., Hashida-Okumura, A. *et al., Biochem. Mol. Biol. Int.* 35(6):1339-1348 (1995), copy of which is attached as Exhibit D for the convenience of the Examiner).

FAD is a small nucleic acid-based molecule. A molecule that is "quite similar" to FAD, as indicated by Hashida-Okumura *et al.*, (e.g., a small nucleic acid based molecule) would not have the requisite characteristics of the claimed agent, as it would be unable to interact with NOS and thereby antagonize autoinhibition by a peptide region of neuronal nitric oxide synthase.

In view of these considerations, Claim 33 is not anticipated by the teachings of Hashida-Okumura *et al.*

Claims 32 and 48-50

The Examiner rejected Claims 32 and 48-50 under 35 U.S.C. 102(e) as being anticipated by Schrader *et al.* (U.S. patent 6,149,936), stating that Schrader *et al.* disclose administration of peptides comprising SEQ ID NO: 4-9 for treating a disease modulated by the production of NOS, so that the antagonism of autoinhibition of eNOS and nNOS is inherent.

Schrader *et al.* describe vectors comprising a DNA sequence encoding iNOS, and use of those vectors for treatment of high blood pressure, arteriosclerosis, stenosis and restenosis. The DNA sequences described by Schrader *et al.* include the entire DNA for coding for the NOS. Schrader *et al.* do not describe administration of proteins or peptides.

The vectors described by Schrader *et al.* increase NOS activity by increasing the entire amount of functioning gene encoding NOS enzyme. They do not activate NOS itself, as required by the claims of the invention: iNOS is not an activator of eNOS or nNOS. NOS activity is increased in Schrader *et al.* merely by increasing the amount of enzyme present, and not by activating existing enzyme. As is usual for any enzyme, activity is proportional to enzyme concentration; this is supported by common practice in the sale of enzymes, which are usually sold by moles or units of activity. Experimental data indicates that once NOS enzyme is in its dimeric state, no self-activation occurs. Furthermore, these vectors are made of *DNA*, and code for the synthesis of the whole enzyme, and not for regulatory regions, not for the production of peptides which regulate existing enzymes in the cells. Thus, they do not anticipate the methods of the invention (e.g., Claims 32 and 49), in which activator *peptides* (and peptidomimetics) are used.

In view of these considerations, Claims 32 and 48-50 are not anticipated by the teachings of Schrader *et al.*

CONCLUSION

In view the amendments and discussion presented above, the application in condition for allowance. Applicants' Attorney respectfully requests that the Examiner reconsider and withdraw all rejections.

If the Examiner believes that a telephone conversation would expedite prosecution of the application, the Examiner is invited to call Elizabeth W. Mata at (915) 845-3558. If Elizabeth W. Mata cannot be reached, the Examiner is invited to call David E. Brook at (978) 341-0036.

Respectfully submitted,

HAMILTON, BROOK, SMITH & REYNOLDS, P.C.

David E. Brook RN 22592

By for Elizabeth W. Mata

Elizabeth W. Mata
Registration No. 38,236
Telephone: (978) 341-0036
Facsimile: (978) 341-0136

Concord, MA 01742-9133
Dated: 5/10/02

OIPE
MAY 1 5 2002
PATENT & TRADEMARK OFFICE

MARKED UP VERSION OF AMENDMENTS

Specification Amendments Under 37 C.F.R. § 1.121(b)(1)(iii)

Replace the paragraph at page 2, lines 15 through page 3, lines 17 with the below paragraph marked up by way of bracketing and underlining to show the changes relative to the previous version of the paragraph.

The current invention concerns recently discovered intrinsic control site elements of constitutive nitric oxide synthases. These intrinsic control site elements, referred to as "regulatory peptides," include the regulatory peptide of endothelial nitric oxide synthase (ENOS), MSGPYNSSPRPEQHKSYKIRFNSVSCSDPLVSSWRRKRK ESSNTD (SEQ. ID. NO. 1); the regulatory peptide of neuronal nitric oxide synthase (NNOS) MRHPNSVQEERKSYKVRFNSVSSYSDSRKSSGDGPDLLRDNFE (SEQ. ID. NO. 2); a polypeptide specific to inducible nitric acid synthase (INOS), [SEQUENCE] amino acids 600-615 of INOS (SEQ. ID. NO. 3). Based on this discovery, methods are now available to identify agents that modulate (activate or inhibit) NOS activity, as well as the agents themselves. Agents include agents that inhibit NOS activity by blocking calmodulin activation of the NOS enzyme; agents that inhibit NOS activity by blocking electron transfer from NADPH to an active site in NOS; agents that activate a constitutive NOS enzyme by antagonizing autoinhibition of a regulatory region of the NOS enzyme; and agents that modulate NOS activity by interacting with the regulatory peptide or spatially adjacent control regions. The agents include the peptides described above, as well as derivatives of these peptides, and homologous peptides. Homologous peptides include substantially isolated peptides having an array of at least two positively charged amino acids, and an amino acid sequence of at least about 60% homology, or about 67% homology, or about 80% homology, or about 90% homology, to the amino acid sequence of the ENOS regulatory peptide; peptides having an amino acid sequence of at least about 60% homology, or about 67% homology, or about 80% homology, or about 90% homology, to the amino acid sequence of the NNOS regulatory peptide; peptides having an amino acid sequence of at least about 60% homology, or about 67% homology, or about 80% homology, or about 90% homology, to the amino acid sequence of the INOS-specific peptide; and peptides having an amino acid sequence of at least about 60% homology, or about 67% homology, or

about 80% homology, or about 90% homology, to the amino acid sequence of the negatively charged loops of the NOS enzymes. The invention further concerns nucleic acids encoding the peptides, derivatives, and homologous peptides; fusions of peptides with proteins or other macromolecules (e.g., polysaccharides); peptidomimetics of the peptides, derivatives, and homologous peptides; and antibodies (either monoclonal or polyclonal antibodies, or fragments thereof) to the peptides, derivatives, and homologous peptides.

Replace the paragraph at page 4, lines 9 through 23 with the below paragraph marked up by way of bracketing and underlining to show the changes relative to the previous version of the paragraph.

The current invention pertains to the discovery of the existence and identity of regulatory peptides of constitutive nitric oxide synthase (NOS) enzymes. As described in the Examples below, Applicant has identified the regulatory peptide of constitutive NOS enzymes as an intrinsic polypeptide insert in the flavin mononucleotide (FMN) binding domain of endothelial nitric oxide synthase (ENOS), MSGPYNSSPRPEQHKSYKIRFNSVSCSDPLVSSWRRKRK ESSNTD (SEQ. ID. NO. 1) and in brain or neuronal nitric oxide synthase (NNOS) MRHPNSVQEERKSYKVRFNSVSSYSDSRKSSGDGPDLLRDNFE (SEQ. ID. NO. 2). Inducible nitric oxide synthase (INOS) lacks a similar polypeptide insert; instead, INOS has an INOS-specific region (the "INOS-specific polypeptide"), amino acids 600-615 of INOS (SEQ. ID. NO. 3), a short loop which is split and greatly extended by the introduction of the regulatory peptide (also referred to herein as the intrinsic peptide) in ENOS and NNOS. Applicant has also identified a core region of the ENOS binding domain: the array of positively charged amino acids, RRKRK [(SEQ ID NO. 7)] (SEQ ID NO: 10), within the ENOS binding domain, alters activity of the enzyme.

Replace the paragraph at page 20, lines 22 through 28 with the below paragraph marked up by way of bracketing and underlining to show the changes relative to the previous version of the paragraph.

These compounds can be manufactured by known methods. For example, a polyester corresponding to the peptide RRKRK (SEQ ID NO: 10) can be prepared by the substituting a hydroxyl group for each corresponding amine group on the R and K amino acids, thereby preparing a

hydroxyacid and sequentially esterifying the hydroxyacids, optionally blocking the basic side chains and acids to minimize side reactions. Determining an appropriate chemical synthesis route can generally be readily identified upon determining the chemical structure using no more than routine skill.

Replace the paragraph at page 29, lines 14 through 24 with the below paragraph marked up by way of bracketing and underlining to show the changes relative to the previous version of the paragraph.

In order to evaluate the functional significance of the putative inhibitory polypeptide, a series of synthetic polypeptides were designed which incorporated structural features of loop regions in the FMN domain. Polypeptides corresponding to promising recognition sites such as the RRKRK (SEQ ID NO: 10) motif were synthesized in lengths ranging from six to thirty five residues, as shown in Table 1, below. Polypeptides corresponding to both the ENOS and NNOS insertions were selected for evaluation. In addition to constructs based on the major insertions, polypeptides corresponding to the neighboring $\alpha>\beta$ loops in all three isoforms were synthesized, because of the possibility that these loops form a significant part of the binding site for the insertion in NOS. This possibility was suggested both by their proximity to the insertion and by their negative charge.

Replace Table 1 on page 30 with the below Table (change is on line 3) marked up by way of bracketing and underlining to show the changes relative to the previous version of the Table.

TABLE 1 Synthetic Peptides

Peptide	Der.[1]	Sequence	SEQ ID NO.
BO58-01	h ENOS	AVDTRLEELGGERT	[21] 35
BO58-02	NNOS	AVDTLLEELGGERT	22
BO58-03	m INOS	DIDQKLSHLGASQT	23
BO58-04	b ENOS	DDVVSLEHET	24

BO58-05	r NNOS	DIVHLEHES	25
BO58-06	m INOS	KASTLEEEQ	26
BO58-07	b ENOS	WRRKRK	12
BO58-08	b ENOS	SSWRRKRKESS	13
BO58-09	h NNOS	QEERKSYKVRF	16
BO58-10	h NNOS	RPEQHKSYKIRF	17
BO58-11	r NNOS	SDSRKSSGDGPDLR	18
JX2	b ENOS	SSPRPEQHKSYKIRFNSVSCSDPLVSSWRRK RKESS	14
JX3	b ENOS	QHKSYKIRFNSVSCSDPLVSSWRRKRKE	15
JX4	h NNOS	QEERKSYKVRFNSVSSYSDSQKSSGDGPDL	19
PEP1		RPEQHKSYKIRF	27
PEP2		QEERKSYKVRFNSVSSYSDSRKSSGDGPDL	28

1 Derivation: h = human; m = mouse; b = bovine and r = rat.

Replace the paragraph at page 32, lines 6 through 8 with the below paragraph marked up by way of bracketing and underlining to show the changes relative to the previous version of the paragraph.

The most effective inhibitory polypeptides contain the motif RRKRK (SEQ ID NO: 10) from the ENOS insertion. Partial inhibition of INOS could also be obtained with NNOS-based polypeptides.

Replace the paragraph at page 33, lines 18 through 24 with the below paragraph marked up by way of bracketing and underlining to show the changes relative to the previous version of the paragraph.

The results of the experiments not only confirmed the function of the major FMN module insertion as the inhibitory polypeptide, but suggested a few details of the switching mechanism. While a number of the polypeptides could modulate CAM binding, the series containing the RRKRK

(SEQ ID NO: 10) [motive] motif was the most instructive. The peptide with three residues following this motif (RRKRKESS) (amino acids 4-11 of SEQ ID NO:13) was a potent CAM antagonist with ENOS and NNOS. CAM binding was decreased almost to background levels, with effects seen at the 10 uM level.

Replace the paragraphs at page 34, lines 1 through 28 with the below paragraphs marked up by way of bracketing and underlining to show the changes relative to the previous version of the paragraphs.

Polypeptides which terminated at the RRKRK (SEQ ID NO: 10) motif, including good inhibitors, were promoters of CAM binding. One polypeptide which had a single amino acid after this motif had no significant effect on CAM binding. Polypeptides based on the flanking loop regions had no significant effect on INOS activity, but tended to weakly promote the binding of CAM to constitutive NOS.

EXAMPLE 4 Mechanism of NOS Control

The results presented here provide powerful evidence that the major insertion in the FMN binding module is the inhibitory polypeptide of constitutive NOS, and that its absence in INOS accounts for the lack of sensitivity of INOS to calcium, and, in part, for its very tight binding of CAM. It appears that INOS has developed from an ancestral constitutive NOS-like protein by loss of the inhibitory peptide. The CAM binding site in INOS and constitutive NOS is apparently related to a similar basic region near the N terminal of P450 reductase, and may have developed from such a region in a common ancestral protein.

The inhibition of INOS by synthetic analogs of the constitutive NOS inhibitory polypeptides is related to the ability of the synthetic polypeptides to modulate CAM binding, but does not have the simple direct relationship expected if the mechanism of peptide inhibitor action was through CAM displacement. The reverse appears to be true: inhibition/activation of NOS at this site is driven by the occupancy of key sites by the inhibitory polypeptide, and CAM binding acts to modify the binding of the intrinsic inhibitory segment to a site or sites nearby on the surface of the enzyme.

It is not necessary to displace CAM in order to inhibit the enzyme at the control site. The data suggest that the binding domain of the inhibitory peptide has several regions. There is at least

one recognition site which binds the RRKRK (SEQ ID NO: 10) motif, and there is indication of a second such site which recognizes sequences such as EERKSYKVRF (amino acids 2-11 of SEQ ID NO: 16) and EQHKSYKIRF (amino acids 3-12 of SEQ ID NO: 17) which occur in the N terminal half of the ENOS and NNOS insertions; peptides which lack RRKRK (SEQ ID NO: 10) but contain these sequences can be inhibitors and/or CAM binding modulators.

Replace the paragraph at page 35, lines 1 through 11 with the below paragraph marked up by way of bracketing and underlining to show the changes relative to the previous version of the paragraph.

Ability to bind to this recognition site does not automatically confer either inhibitory character or the ability to prevent CAM binding. It is apparent that CAM binding is strongly inhibited by peptides with a short extension after the RRKRK (SEQ ID NO: 10) motif; a three residue extension produced a peptide which reduced CAM binding to near background levels, while even a single residue produced a small decrease. The ability of the two polypeptides which ended in the RRKRK (SEQ ID NO: 10) motif to potentiate CAM binding strongly suggests that a region of overlap between the CAM binding site and the peptide binding site exists, in which the overlap occurs between bound CAM and residues towards the C terminal from RRKRK (SEQ ID NO: 10) . In the intrinsic peptide other residues may contribute to the overlap, since it is both larger and more conformationally constrained than the synthetic analogs used here as probes.

Claim Amendments Under 37 C.F.R. § 1.121(c)(1)(ii)

31. (Amended) A method of activating endothelial nitric oxide synthase, comprising contacting the endothelial nitric oxide synthase with an effective amount of an [agent of Claim 16] activator of endothelial nitric oxide synthase which antagonizes autoinhibition by a peptide region of endothelial nitric oxide synthase, wherein the region is between about amino acids 590-650 of endothelial nitric oxide synthase.

32. (Amended) A method of activating endothelial nitric oxide synthase, comprising contacting the endothelial nitric oxide synthase with an effective amount of [an agent of Claim 19] a

constitutive nitric oxide synthase activator peptide comprising an amino acid sequence selected from the group consisting of: SEQ ID NO. 4, SEQ ID NO. 5, SEQ ID NO. 6, SEQ ID NO. 7, SEQ ID NO. 8, SEQ ID NO. 9, and activating fragments and derivatives of SEQ ID NO. 4, SEQ ID NO. 5, SEQ ID NO. 6, SEQ ID NO. 7, SEQ ID NO. 8, SEQ ID NO. 9.

33. (Amended) A method of activating neuronal nitric oxide synthase, comprising contacting the neuronal nitric oxide synthase with an effective amount of an [agent of Claim 20] activator of neuronal nitric oxide synthase which antagonizes autoinhibition by a peptide region of neuronal nitric oxide synthase, wherein the region is between about amino acids 820-880 of neuronal nitric oxide synthase.

48. (Amended) A method of treating a disease modulated by production of nitric oxide by endothelial nitric oxide synthase in a mammal, comprising administering to the mammal an effective amount of an [agent of Claim 16] activator of endothelial nitric oxide synthase which antagonizes autoinhibition by a peptide region of endothelial nitric oxide synthase, wherein the region is between about amino acids 590-650 of endothelial nitric oxide synthase.

49. (Amended) A method of treating a disease modulated by production of nitric oxide by endothelial nitric oxide synthase in a mammal, comprising administering to the mammal an effective amount of [an agent of Claim 19] a constitutive nitric oxide synthase activator peptide comprising an amino acid sequence selected from the group consisting of: SEQ ID NO. 4, SEQ ID NO. 5, SEQ ID NO. 6, SEQ ID NO. 7, SEQ ID NO. 8, SEQ ID NO. 9, and activating fragments and derivatives of SEQ ID NO. 4, SEQ ID NO. 5, SEQ ID NO. 6, SEQ ID NO. 7, SEQ ID NO. 8, SEQ ID NO. 9.

50. (Amended) A method of treating a disease modulated by production of nitric oxide by neuronal nitric oxide synthase in a mammal, comprising administering to the mammal an effective amount of an [agent of Claim 20] activator of neuronal nitric oxide synthase which

antagonizes autoinhibition by a peptide region of neuronal nitric oxide synthase, wherein the region is between about amino acids 820-880 of neuronal nitric oxide synthase.

EXHIBIT A

THE JOURNAL OF BIOLOGICAL CHEMISTRY
Vol. 272, No. 47, Issue of November 21, pp. 29769–29777, 1997
Printed in U.S.A.
© 1997 by The American Society for Biochemistry and Molecular Biology, Inc.

An Autoinhibitory Control Element Defines Calcium-regulated Isoforms of Nitric Oxide Synthase*

(Received for publication, March 31, 1997, and in revised form, August 25, 1997)

John C. Salerno‡, Dawn E. Harris‡§, Kris Irizarry‡, Binesh Patel‡, Arturo J. Morales‡, Susan M. E. Smith¶, Pavel Martasek‖, Linda J. Roman‖, Bettie Sue S. Masters‖, Caroline L. Jones, Ben A. Weissman**, Paul Lane**, Qing Liu§**‡‡, and Steven S. Gross**‡‡§§**

*From the ‡Department of Biology, Rensselaer Polytechnic Institute and ¶Aeneas Biotechnology, Troy, New York 12180, ‖Department of Biochemistry, The University of Texas Health Science Center, San Antonio, Texas 78284-7760, **Department of Pharmacology, Cornell University Medical College, New York, New York 10021, and ‡‡Program in Biochemistry and Structural Biology, The Cornell University Graduate School of Medical Sciences, New York, New York 10021*

Nitric oxide synthases (NOSs) are classified functionally, based on whether calmodulin binding is Ca^{2+}-dependent (cNOS) or Ca^{2+}-independent (iNOS). This key dichotomy has not been defined at the molecular level. Here we show that cNOS isoforms contain a unique polypeptide insert in their FMN binding domains which is not shared with iNOS or other related flavoproteins. Previously identified autoinhibitory domains in calmodulin-regulated enzymes raise the possibility that the polypeptide insert is the autoinhibitory domain of cNOSs. Consistent with this possibility, three-dimensional molecular modeling suggested that the insert originates from a site immediately adjacent to the calmodulin binding sequence. Synthetic peptides derived from the 45-amino acid insert of endothelial NOS were found to potently inhibit binding of calmodulin and activation of cNOS isoforms. This inhibition was associated with peptide binding to NOS, rather than free calmodulin, and inhibition could be reversed by increasing calmodulin concentration. In contrast, insert-derived peptides did not interfere with the arginine site of cNOS, as assessed from [^{3}H]N^G-nitro-L-arginine binding, nor did they potently effect iNOS activity. Limited proteolysis studies showed that calmodulin's ability to gate electron flow through cNOSs is associated with displacement of the insert polypeptide; this is the first specific calmodulin-induced change in NOS conformation to be identified. Together, our findings strongly suggest that the insert is an autoinhibitory control element, docking with a site on cNOSs which impedes calmodulin binding and enzymatic activation. The autoinhibitory control element molecularly defines cNOSs and offers a unique target for developing novel NOS activators and inhibitors.

Nitric oxide is a ubiquitous cell-signaling molecule, with protean roles in physiology and pathophysiology (1–3). Encoded by distinct genes, mammalian NO synthases (NOSs)[1] comprise a family of three calmodulin-dependent biopterohemoflavoproteins that are functionally distinguished by their modes of regulation (4). The two constitutively expressed isoforms of NOS (cNOSs), first identified in neuronal cells (nNOS) and endothelial cells (eNOS), remain dormant until calcium/calmodulin (Ca^{2+}/CaM) binding is actuated by transient elevations in intracellular Ca^{2+}. This Ca^{2+}-dependent mode of regulation provides pulses of NO for moment-to-moment modulation of vascular tone and neurosignaling. In contrast, activity of the immunostimulant-induced isoform of NOS (iNOS) is Ca^{2+}-independent, providing continuous high output NO generation for host defense. A remarkably high affinity for CaM, even at basally low levels of intracellular calcium, is responsible for the Ca^{2+} independence of iNOS (5).

Whether a given NOS isoform binds CaM in a Ca^{2+}-dependent or -independent manner has been assumed to be a property solely of the amino acid sequence specified by a 20–25-amino acid CaM binding site. However, this restrictive view is challenged by findings that chimeric eNOS and nNOS, which have had their CaM binding sequences replaced with the corresponding sequence from iNOS, still require Ca^{2+} for full activity (6, 7). Because regulation of enzyme systems by Ca^{2+}/CaM typically involves displacement of an intrinsic autoinhibitory polypeptide (8, 9), we hypothesized that the binding of Ca^{2+}/CaM to cNOSs may similarly trigger activation by displacing a control element. Here we identify a multiple amino acid insertion which serves as a control element unique to cNOSs and which molecularly defines Ca^{2+}-dependent isoforms of NOS.

EXPERIMENTAL PROCEDURES

Protein Modeling—Molecular modeling of the FMN binding module of nitric oxide synthase isoforms was done using the Insight and Homology programs from Biosym (BIOSYM/Molecular Simulations, San Diego, CA) running on a silicon graphics Indigo2 workstation. After alignment of NOS sequences with homologous FMN binding proteins of known structure (see "Results"), structurally conserved region (SCR) boxes were created corresponding to conserved regions of secondary structure and regions involved directly in FMN binding. These regions were characterized by high positive scores as evaluated by Dayhoff's mutation matrix (10). After assignment of coordinates in the SCR regions, the loop regions between the SCR boxes were modeled by searching the Brookhaven protein data base. The crude model structure was relaxed to a sterically and energetically reasonable state using the Discover program (BIOSYM/Molecular Simulations) for molecular me-

* This work was supported in part by National Institutes of Health Grants HL 50656 and HL 44603 (to S. S. G.), HL 30050 and GM52419 (to B. S. S. M.), and a grant from the Robert A. Welch Foundation (to B. S. S. M.). The costs of publication of this article were defrayed in part by the payment of page charges. This article must therefore be hereby marked "*advertisement*" in accordance with 18 U.S.C. Section 1734 solely to indicate this fact.

§ These authors contributed equally to the work.

§§ To whom correspondence should be addressed: Dept. of Pharmacology, Cornell University Medical College, 1300 York Ave., New York, NY 10021. Tel.: 212-746-6257; Fax: 212-746-8835; E-mail: ssgross@med.cornell.edu.

[1] The abbreviations used are: NOS, nitric oxide synthase; cNOS, calcium-dependent NOS, iNOS, calcium-independent NOS; eNOS, the endothelial isoform of cNOS; nNOS, the neuronal isoform of cNOS; CaM, calmodulin, SCR, structurally conserved region; CPR, cytochrome P450 reductase; DTT, dithiothreitol.

The material on this page was copied from the collection of the National Library of Medicine by a third party and may be protected by U.S. Copyright law.

chanics and dynamics calculations. This includes splice repair to remove unrealistic structural features at SCR-loop junctions, end repair to assign reasonable structures to C-terminal and N-terminal extensions, and structural optimization to remove steric overlaps and to reduce the structure to a energetic minimum. Energy minimizations were begun using the steepest descent method; this was replaced by conjugate gradient method as convergence was approached.

Purification of NOS Isoforms—Rat neuronal cNOS (nNOS) and bovine endothelial cNOS (eNOS) were purified from *Escherichia coli* harboring pGroELS and pCW vector expression systems for nNOS and eNOS, as described previously (11, 12). iNOS-rich cytosol was prepared from rat aortic smooth muscle cells, which were isolated from Fisher rat thoracic aortae (13) and grown in 75-cm^2 culture flasks at passage 10–15. Cells were stimulated for 16 h in culture medium containing a combination of lipopolysaccharide (30 μg/ml) and rat recombinant interferon-γ (50 ng/ml), washed twice with 10 ml of ice-cold phosphate-buffered saline, and harvested with a Teflon cell scraper into an additional 10 ml of iced phosphate-buffered saline. Cell suspensions were centrifuged at 800 × *g* for 10 min, resuspended in 100 μl/75-cm^2 culture flask of ice-cold distilled H_2O containing a mixture of protease inhibitors (pepstatin 10 μg/ml, leupeptin 10 μg/ml, and phenylmethylsulfonyl fluoride 100 μM) and lysed by three cycles of freezing in liquid nitrogen and thawing in a 37 °C water bath. Lysates were centrifuged at 100,000 × *g* for 1 h, and supernatants were stored at −70 °C until use.

NOS Activity Measurement—NOS activity was measured in 96-well microtiter plates at 25 °C based on the kinetics of NADPH consumption or the oxidation of Fe^{2+}-myoglobin to Fe^{3+}-myoglobin, as described previously (14). For NADPH consumption measurements, incubation mixtures contained 50 mM Tris-HCl (pH 7.60), 100 μM $CaCl_2$, 10 μM tetrahydrobiopterin, 500 μM NADPH, 500 μM L-arginine, 1 mM DTT, 1 μM calmodulin, pH 7.6, and the indicated concentration of peptide in a final volume of 100 μl. Reactions were initiated by the addition of 20 pmol of nNOS, 10 pmol of eNOS, or 15 μg of rat iNOS-rich cytosol. NADPH consumption was determined from the rate of decrease in A_{340}, measured at 15-s intervals for a period of 30 min in a kinetic microplate spectrophotometer (Molecular Devices; Menlo Park, CA). The rate of decline in A_{340} measured when NOS was omitted from incubates was subtracted from all values. Samples in which iNOS activity was measured based on Fe^{2+}-myoglobin oxidation were prepared as above, but additionally contained 15 μg of rat iNOS-rich cytosol and a final concentration of 40 μM Fe^{2+}-myoglobin. Preparation of Fe^{2+}-myoglobin and spectrophotometric measurement of its rate of oxidation to Met-myoglobin by NO, was as described earlier (14).

^{125}I-Calmodulin Binding Measurement—Calmodulin was labeled with ^{125}I to a specific activity of 25–150 μCi/g, using the Bolton-Hunter method (15). ^{125}I-Calmodulin binding assays were performed in triplicate using 96-well microfiltration plates with GFB filter bottoms (Millipore, Bedford, MA). Before use, filters were preincubated for 1–2 min with 100 μl of buffer containing 50 mM Tris-HCl, pH 7.6, 1 mM DTT, 100 μM $CaCl_2$, and 0.5 mg/ml β-lactoglobulin; buffer was then removed by vacuum filtration. Binding reactions were comprised of: 50 mM Tris-HCl, pH 7.6, 1 mM DTT, 0.5 mg/ml β-lactoglobulin, 100 μM $CaCl_2$, 10 μM tetrahydrobiopterin, 1 nM ^{125}I-CaM (2500–5000 cpm) and 1–2 pmol of NOS in a 100-μl total volume. Samples were incubated for 15 min at 23 °C, and binding was quickly terminated by vacuum filtration. Filters were washed twice with 100 μl of ice-cold buffer containing 50 mM Tris-HCl, pH 7.6, and 100 μM $CaCl_2$ and air-dried. Scintillation mixture was added to each well (25 μl; OptiPhase SuperMix, Wallac Inc., Gaithersburg, MD), and plates were counted in a Microbeta Plus liquid scintillation counter (Wallac Inc.). Nonspecific binding was determined in samples that additionally contained 10 mM EGTA. In studies of the effect of inhibitory effect of peptide inhibitors on ^{125}I-CaM binding to NOS, blank binding was determined in the presence of peptide and absence of NOS. Dissociation of ^{125}I-CaM was similarly monitored in 96-well filtration plates. ^{125}I-CaM·nNOS complexes were first produced by incubation of 2 pmol of nNOS, 1 nM of ^{125}I-CaM, 100 μM $CaCl_2$, 10 μM tetrahydrobiopterin, 50 mM Tris-HCl, pH 7.6, 1 mM DTT, and 0.5 mg/ml β-lactoglobulin for 15 min (23 °C). To initate dissociation, a 3000-fold excess of unlabeled CaM (3 μM) was added at time 0, with or without simultaneous addition of the indicated concentration of bovine $eNOS^{607-634}$.

[^{3}H]N^GNitro-L-arginine Binding Measurement—Assays of [^{3}H]N^G-nitro-L-arginine binding were performed in 96-well polyvinylidene difluoride microfiltration plates (Millipore, Bedford, MA) as described previously (16), using 5 pmol of nNOS and the indicated concentrations of NOS-derived peptides.

Calcineurin Activity Measurement—Activity of the calmodulin-dependent phosphatase calcineurin (protein phosphatase 2B) was monitored in a 96-well kinetic microplate spectrophotometer at 37 °C, based on rate of hydrolysis of the artificial substrate *p*-nitrophenyl phosphate (17). Incubation mixtures contained 50 mM Tris-HCl, pH 7.6, 100 nM bovine brain calmodulin, 40 mM *p*-nitrophenyl phosphate, 400 μM $CaCl_2$, and 0.1% 2-mercaptoethanol in a 100-μl total volume. Reactions were initiated by the addition of 20 pmol of calcineurin, and activity was monitored continually at A_{405} for 60 min at 15-s intervals. Assay blanks additionally contained 10 mM EGTA, resulting in >90% inhibition of activity.

Proteolysis of NOS Isoforms—Limited proteolysis was performed on incubates containing 40 pmol of recombinant nNOS purified from stably transfected HEK-293 cells (11) or 50 pmol of recombinant eNOS purified from *E. coli* (12). Samples were preincubated at room temperature for 15 min in a 100-μl volume containing: 50 mM Tris, pH 7.6, 1 mM DTT, 10 μM CaM, 100 μM $CaCl_2$, with or without 10 mM EGTA. Proteolysis was initiated by the addition of 20 microunits of L-1-tosylamido-2-phenylethyl chloromethyl ketone-immobilized trypsin (Sigma) per pmol of NOS. Samples (25 μl) were collected after 0, 5, 10, and 20 min, and proteolysis was terminated by boiling with an equal volume of 2 × SDS gel-loading buffer. Peptide products were resolved on an 8–16% gradient SDS-polyacrylamide gel electrophoresis and visualized by staining with Coomassie Blue. Accurate molecular mass determination of tryptic fragments was performed by mass spectrometry at the Rockefeller University Protein/DNA Biotechnology Center, using matrix-assisted laser desorption and time of flight detection (Perseptive Biosystems Inc., Framingham, MA). For N-terminal sequence analysis, tryptic digests were prepared as above and subject to SDS-polyacrylamide gel electrophoresis, but then electrotransfered to polyvinylidene difluoride membranes. Amino acid sequencing was performed on an Applied Biosystems 477A protein sequencer.

Peptides—Synthetic peptides were obtained from SynPep (Dublin, CA) and other commercial suppliers. Purity was evaluated by high performance liquid chromatography and mass spectroscopy and exceeded 80% in all cases with typical purity ≈90%. Predominant impurities differed from the desired products by one amino acid residue, resulting from incompletely coupled synthesis.

Chemicals—Rat recombinant interferon-γ, RPMI culture medium, and cell culture reagents were from Life Technologies, Inc. Radioisotopes were from Dupont NEN, lipopolysaccharide (*E. coli* serotype 0111:B4), chemicals, and L-1-tosylamido-2-phenylethyl chloromethyl ketone-immobilized trypsin were obtained from Sigma, calmodulin was from Calbiochem, and tetrahydrobiopterin was from Schirks Laboratories (Jona, Switzerland). Enzymes were purchased from Pharmacia LKB Biotechnology, Promega, or New England Biolabs.

RESULTS AND DISCUSSION

Nitric oxide synthases are large multidomain enzymes in which a series of gene fusion events has resulted in the incorporation of modules showing significant homology to smaller ancestral proteins (18, 19). NOSs can be coarsely dissected into an N-terminal oxygenase domain and a C-terminal reductase domain, bridged by a canonical binding sequence for CaM (20). Calmodulin binding initiates electron transfer between the reductase and catalytic domains, thereby activating catalysis (21). The oxygenase domains have binding sites for substrate (arginine), heme, and tetrahydrobiopterin, whereas the reductase domain has binding sites for FAD, FMN, and NADPH.

Bredt *et al.* (22) were first to reveal the homology between the C-terminal half of NOS and NADPH-cytochrome P450 reductase (CPR), noting conserved regions corresponding to FMN, FAD, and NADPH binding domains. The FMN-binding modules of NOS isoforms and CPR are in turn highly homologous to the flavodoxins, which are small FMN-binding proteins that function as electron carriers in bacteria (23). The FAD and NADPH binding domains are closely related to chloroplast ferredoxin-$NADP^+$ reductase and other related proteins.

Sequence Alignments—Five flavodoxins have been crystallized and solved by x-ray diffraction (24). Three regions in these flavodoxins are involved in binding the FMN prosthetic group; the first of these is close to the N terminus, and is immediately proceeded by the initial β strand of the structure. Although only one of these FMN binding regions was identified in nNOS by Bredt *et al.* (22), each of them has a corresponding homolog

The material on this page was copied from the collection of the National Library of Medicine by a third party and may be protected by U.S. Copyright law.

```
                                    INITIAL FMN BINDING REGION
NCPR_HUMAN  ESSFVEKMKK TGRNIIVFYG SQTGTAEEFA NRLSKD.AHR YGMRGMSADP  115
NOSE_BOVIN  GTLMAKRV.. ...KATILYA SETGRAQSYA QQLGRLFRKA FDPRVLCMD.  556
  NOSB_RAT  GQAMAKRV.. ...KATILYA TETGKSQAYA KTLCEIFKHA FDAKAMSME.  789
NOSM_MOUSE  RKVMASRV.. ...RATVLFA TETGKSEALA RDLATLFSYA FNTKVVCMD.  567
FLAV_ECOLI  .......... ..AITGIFFG SDTGNTENIA KMIQKQL.GK .D.VADVHDI   35
FLAV_DESVH  .......... .MPKALIVYG STTGNTEYTA ETIARELADA .GYEVDSRDA   38

                          FLANKING LOOP   SECOND FMN SITE
NCPR_HUMAN  EEYDLADLSS LPEIDNALVV FCMATYGEGD PTDNAQDFYD WL.QE.....  159
NOSE_BOVIN  .EYDVVSL.. ...EHETLVL VVTSTFGNGD PPENGESFAA AL.MEMSGPY  599
  NOSB_RAT  .EYDIVHL.. ...EHEALVL VVTSTFGNGD PPENGEKFGC AL.MEMRHP.  831
NOSM_MOUSE  .QYKASTL.. ...EEEQLLL VVTSTFGNGD CPSNGQTLKK SLFML.....  606
FLAV_ECOLI  AKSSKEDL.. ...EAYDILL LGIPTWYYGE ....AQCDWD DF.FP.....   70
FLAV_DESVH  ASVEAGGLF. ...EGFDLVL LGCSTWGDDS IE..LQDDFI PL.FD.....   76

                    LOCATION OF REGULATORY LOOP INSERT
NCPR_HUMAN  .......... .......... .......... ..........TDVDLSGVKF  169
NOSE_BOVIN  NSSPRPEQHK SYKIRFNSVS CSDPLVSSWR RKRKESSNTD SAGAGTLRFL  649
  NOSB_RAT  NS..VQEERK SYKVRFNSVS SYSDSRKSSG DGPDLRDNFE STGPLANVRF  879
NOSM_MOUSE  .......... .......... .......... .......... .RELNHTFRY  615
FLAV_ECOLI  .......... .......... .......... ........TL EEIDFNGKLV   82
FLAV_DESVH  .......... .......... .......... ........SL EETGAQGRKV   88

                    THIRD FMN SITE  FLANKING LOOP
NCPR_HUMAN  AVFGLGNKT. Y.EHFNAMGK YVDKRLEQLG AQRI  201
NOSE_BOVIN  CVFGLGSRA. Y.PHFCAFA. AVDTRLEELG GERL  680
  NOSB_RAT  SVFGLGSRA. Y.PHFCAFGH AVDTLLEELG GERI  911
NOSM_MOUSE  AVFGLGSSM. Y.PQFCAFAH DIDQKLSHLG ASQL  647
FLAV_ECOLI  ALFGCGDQED YAEYFCDALG TIRDIIEPRG ATIV  116
FLAV_DESVH  ACFGCGDSS. Y.EYFCGAVD AIEEKLKNLG AEIV  120
```

FIG. 1. **Structure-based sequence alignment of FMN binding domains of human NADP$^+$-cytochrome 450 reductase (*NCPR_HUMAN*), bovine eNOS (*NOSE_BOVIN*), rat nNOS (*NOSB_RAT*), mouse iNOS (*NOSM_MOUSE*) and flavodoxins from *E. coli* (*FLAV_ECOLI*), and *D. vulgaris* (*FLAV_DESVH*).** Complete sequences were obtained from the Swiss Protein data base using the given designations. Alignment was performed manually by aligning the flavin binding sequences and conserved secondary structural elements from flavodoxin crystal structures as evaluated with Biosym's Homology software. The C-terminal end of the domain (≈35 residues for *Desulfovibrio* sequence) is omitted to conserve space.

in NOSs. The first step in alignment of the NOS FMN binding domain with the flavodoxins was the identification of these regions in each NOS isoform. This was followed by the identification of conserved secondary structural elements in NOS, primarily by their homology to the corresponding elements in flavodoxins by mutation matrix criteria (10).

Fig. 1 shows alignment of a select set of NOS, CPR, and bacterial flavodoxin sequences, illustrating the conservation of regions involved in FMN binding. It is obvious that a major insertion of ≈45 amino acids has occurred in mammalian cNOSs. A corresponding insert is also found in the FMN binding region of the cloned invertebrate cNOSs from *Rhodnius prolixus* (25) and *Drosophila melanogaster* (26); these inserts are somewhat larger (54–63 amino acids), but contain regions of marked homology to mammalian cNOS inserts. Expanding this alignment to include dozens of known flavodoxins and related FMN-containing flavoproteins reveals that only cNOSs exhibit such an insertion. Moreover, the corresponding region of iNOS sequences closely resemble flavodoxin sequences but lack an insert anywhere within the FMN binding domain. Therefore, occurrence of the amino acid insertion correlates with Ca^{2+}/CaM control. This insertion represents the single most prominent difference between cNOSs and iNOS amino acid sequences, considered over their entire length.

The cNOS FMN module insertions are notably rich in charged residues and have an excess of positive charge. This is especially true of the eNOS isoform, which contains the motif RRKRK. Considerable homology exists between the cNOS insertions, particularly toward their N termini. It is also apparent that some structural reorganization has taken place during evolution, which may allow the two or three positively charged residues (depending on species) in the nNOS equivalent of the RRKRK region to recognize a similar binding site. The pattern of conservation suggests that eNOS and nNOS insertions contain at least two motifs.

Structural Models—The availability of solved x-ray crystal structures for flavodoxins allows us to position the insertion in three dimensions relative to the calmodulin binding site. Homology-based molecular models have been constructed for the FMN binding domains of cNOSs, iNOS, and CPR, which could be relaxed to a sterically and energetically reasonable state. After relaxation of these FMN binding domain models, no steric overlaps were present, and energies were approximately −300 kcal, comparable or lower than that of reference flavodoxin crystal structures.

As shown in Fig. 2 (*upper left*), the backbone structure of iNOS and CPR are virtually superimposable on the backbone of *Desulfovibrio vulgaris* flavodoxin, the closest solved structural homolog of the FMN binding modules of the NOS isoforms.[2] The structure, a Rossmann fold motif (28), is a five stranded parallel β-sheet with the FMN binding site along one edge. Homology predicts that two aromatic residues in murine iNOS, Phe^{587} and Tyr^{625}, are in contact with the FMN ring system; Tyr^{625} serves as a shielding residue.

Fig. 2 (*upper right*) shows the corresponding backbone structure of eNOS; nNOS is extremely similar but not shown. Most of the eNOS backbone can be superimposed on homologs shown in Fig. 2 (*upper left*), with the insertion projecting from the upper edge of the sheet opposite the FMN binding site. Structurally, it corresponds to the replacement of a tight 5–10 residue $\alpha \rightarrow \beta$ loop with an ≈50-residue structure about one-third the size of the entire FMN binding module. We are unable to propose a conformation for the insertion because we lack a solved homolog; the structure shown is merely intended to convey relative position and size.

The CaM binding site is immediately adjacent to the N-terminal edge of the FMN binding domain (painted *white* in Fig. 2, *upper left*). With CaM bound, the CaM recognition site would predictably be in a helical conformation (29, 30); steric constraints suggest that it extends almost directly away from the FMN binding domain. The *lower panels* of Fig. 2 show models of the FMN binding domains of iNOS (*left*) and eNOS (*right*) with CaM (*yellow* ribbon; based on Vorherr *et al.* (30)) positioned above the N-terminal strand of the FMN domain. There are 7–8 residues between the end of the CAM recognition site proper and the start of the initial strand of the β-sheet; 2–3 residues at each end of this short linker are needed to clear the van der Waals surfaces of CaM and the FMN domain. This leaves 2–3 residues that are conformationally unrestricted, and, hence, there are uncertainties about the exact position above the β-sheet of CaM and the orientation of the axis of the CaM recognition site. The position of CaM relative to the FMN domain is unspecified with respect to rotations about the *y* axis of Fig. 2 by available information (corresponding to the axis of

[2] Recently, the crystal structure of NADPH-cytochrome P450 oxidoreductase has been reported at 3.0 Å resolution (27). The FMN-binding module bears striking homology to *D. vulgaris* flavodoxin.

The material on this page was copied from the collection of the National Library of Medicine by a third party and may be protected by U.S. Copyright law.

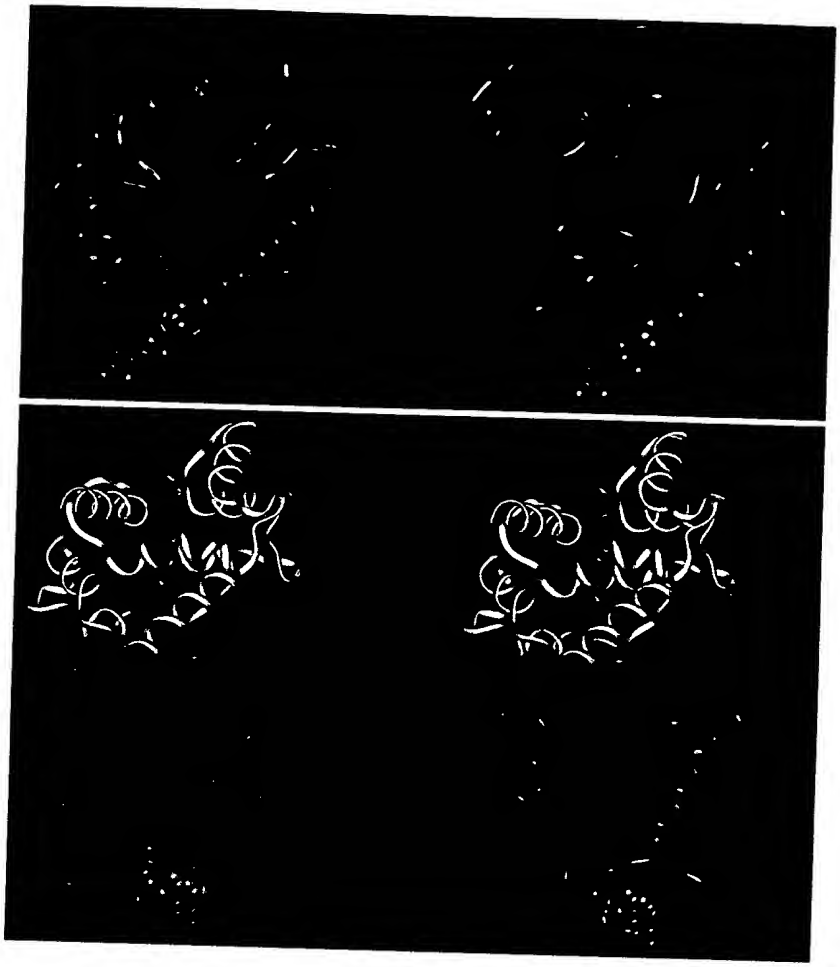

FIG. 2. **Structural models of FMN binding domains.** *Upper left panel*, flavodoxin (*silver*; from McMillan *et al.* (11)), cytochrome P450 reductase (*gold*; homology model), rat iNOS (*cyan*, homology model). *Upper right panel*, bovine eNOS (*pink*, with autoinhibitory peptide in *gold*; homology model). N-terminal residues of NOS isoform domains are depicted in *white* with the CaM binding site directly above this point. FMN is shown in space filling representation at *bottom*. Central β-sheets and flanking α-helices are visible in all structures. *Lower panels*, approximate location of bound CaM (*yellow*, with NOS CaM binding sequence in *blue*) relative to FMN binding domain (*pink*, with FMN in *gold* space-filling rendering) of rat iNOS (*left*) and bovine eNOS (*right*).

the CaM-binding helix of *lower panels*). It is notable that calmodulins (molecular mass $\approx$ 17 kDa) are larger than the entire FMN-binding module. Although the insertion is midway through the sequence of the FMN-binding module, in three dimensions the model predicts it to be directly adjacent to the CaM binding site. The model predicts also that CaM binding would be sterically hindered by the insertion, suggesting that the insertion can exist in more than one physiologically relevant conformation.

Two aspects of this model strongly suggest that the insert functions as a control element, 1) the correlation between Ca^{2+}/CaM control and the presence of the insertion and 2) the proximity of the CaM binding site to the insertion and the probable steric interactions which would ensue. An attractive potential role for the insert is that of an inhibitory polypeptide which is displaced by CaM binding. It differs from inhibitory polypeptides common to other CaM-dependent enzymes, and CaM itself, in its lack of acidic and hydrophobic amino acids; this makes direct binding of the insertion to CaM sites in NOS isoforms unlikely. Nonetheless, CaM could conceivably displace the polypeptide insert from a neighboring site by binding domain overlap or through allosteric effects.

Synthetic Polypeptide Effects on NOS Activity—Functional significance of the putative autoinhibitory insert of cNOSs was evaluated using a series of synthetic polypeptide fragments. Polypeptides corresponding to promising recognition sites such as the RRKRK motif of the eNOS insert were synthesized in lengths ranging from 6 to 33 residues, as shown in Table I. Both eNOS- and nNOS-derived peptide fragments were evaluated; effects on NOS activity are summarized in Table II. At concentrations of 50–100 μM, several polypeptide fragments of the cNOS insertions profoundly inhibited eNOS and nNOS activity. The most effective inhibitory polypeptides were from the eNOS insertion and contained the RRKRK motif (Table II and Fig. 3*A*). Human nNOS-derived polypeptides weakly inhibited eNOS, but were without effect on nNOS. While all peptides were less potent on iNOS, significant inhibition was obtained with $eNOS^{601-633}$ and $eNOS^{607-634}$. Notably, inhibition of iNOS activity by these peptides was rapid and apparently complete within one minute of addition. Because CaM is very tightly bound to iNOS and has a remarkably slow off-rate, with little dissociation occurring even after boiling (5), inhibition probably occurs without CaM displacement.

Synthetic Polypeptide Effects on Calmodulin Binding—Overlap of the cNOS polypeptide insert and the CaM recognition site, suggested from molecular modeling, implies that the insert may obstruct CaM binding. If this involves "docking" of the insert within cNOSs, synthetic homologs of the insert might similarly bind and interfere with CaM binding. As shown in Table II, potent inhibition of ^{125}I-CaM binding to nNOS was observed with insert-derived polypeptide fragments; relative peptide potency for inhibiting CaM binding mirrored that for blocking nNOS activation. IC_{50} values for eNOS-derived peptide fragments ranged from 1 to 10 μM, and potency increased as the RRKRK motif was progressively lengthened to include up to 33 amino acids (Fig. 3*B*). Inhibition of nNOS activity and CaM binding by insert-derived peptides was fully reversed by excess CaM (see Fig. 3, *C* and *D*, for findings with $eNOS^{607-634}$), indicative of a competitive mode of inhibition. Thus, the greater apparent potency of peptides for inhibiting CaM binding *versus* activity, indicated in Table II, is explained by differences in assay conditions; lower CaM concentrations

The material on this page was copied from the collection of the National Library of Medicine by a third party and may be protected by U.S. Copyright law.

were used to assess binding (1 nM) *versus* activity (100 nM). Inhibition of CaM binding by peptide could not be overcome by excess Ca^{2+} (Fig. 3*E*).

Conceivably, the synthetic peptides could interfere with CaM binding to NOS by interacting with either NOS or CaM itself. That NOS is the actual binding target for eNOS-derived insert peptides is indicated by several findings. First, direct binding of peptide to ^{125}I-CaM, quantified in the absence of NOS, was undetectable at concentrations that inhibited >90% of CaM binding to nNOS (data not shown). Second, the CaM-dependent phosphatase calcineurin, which resembles cNOSs in having a K_d for CaM of 5 nM (31), was not inhibited by concentrations of insert-derived peptides that potently inhibit nNOS activity (see Fig. 4). Third, eNOS-derived peptides markedly enhanced the dissociation rate of ^{125}I-CaM from preformed complexes with nNOS (Fig. 3*D*). In this experimental setting, dissociated ^{125}I-CaM is prevented from reassociating with NOS by addition of a 3,000-fold molar excess of unlabeled CaM. Thus, in order for a synthetic eNOS-derived peptide to *eject* CaM from its binding site on nNOS, it must at least transiently form a ternary CaM-containing complex with NOS. Conceivably, this transient ternary complex could involve interactions of peptide with CaM as well as NOS. These findings suggest that the binding domain of the putative eNOS autoinhibitory element on nNOS either overlaps or allosterically perturbs the CaM binding domain.

Previously described inhibitors with demonstrated selectivity for NOS influence the arginine site in a manner that can be detected as a loss in sites or binding affinity for the arginine analog, [^{3}H]N^G-nitro-L-arginine. Thus, it is notable that the cNOS insert peptides inhibit NOS activity and CaM binding with a slight increase, rather than decrease, in [^{3}H]N^G-nitro-L-arginine binding (Table II). Specificity of the insert peptides is also indicated by a lack of inhibition of either NOS activity or CaM binding with each of five synthetic peptides, 10–15 amino acids in length, derived from sites on the FMN binding domain of cNOSs, which are distinct from the insert polypeptide (not shown).

Effects of Calmodulin on Exposure of the Insert—Displacement of the insert peptide from an internalized binding site on cNOSs by CaM would conceivably enhance exposure of the insert to proteolysis. This hypothesis was tested by examining the pattern of peptide accumulation during limited trypsinolysis of both nNOS and eNOS, in the absence and presence of bound CaM (Fig. 5).

Earlier, Sheta *et al.* (20) showed that of 165 possible tryptic cleavage sites in rat nNOS, a single preferred cut site resides at Arg^{727} within the CaM binding sequence. Cutting at this site has served as an effective means for isolation of distinct reductase and oxygenase domains. With CaM present but not bound (due to addition of the Ca^{2+}-chelator, EDTA; see Fig. 5*A*), we similarly observe that tryptic cleavage of nNOS occurs almost exclusively at a single site, consistent with Arg^{727} within the CaM binding site. Accordingly, we found a time-dependent accumulation of fragments with apparent molecular masses of 77 and 85 kDa, corresponding to C-terminal reductase and N-terminal oxygenase domains, respectively (Fig. 5*A*). When CaM was permitted to bind nNOS, by omission of EDTA, Arg^{727} was protected from proteolysis, and a novel tryptic cleavage site was revealed. Cutting at this new site yielded fragments of apparent molecular masses of 63 and 93 kDa (Fig. 5*A*). Molecular mass refinement by matrix-assisted laser desorption ionization spectrometry indicated the smaller fragment to be 64,809 ± 324 Da. This product is best explained by cleavage at Arg^{855}–Lys^{856}, a dibasic (RK) site within the insert peptide which predicts a C-terminal fragment of 65,071 Da. That this fragment originates from the C terminus of nNOS is indicated by our finding that it is the predominant trypsinolysis product of the bacterial-expressed C-terminal reductase domain ($nNOS^{721–1429}$) but is not produced by trypsinolysis of the N-terminal oxygenase domain ($nNOS^{1–721}$) (data not shown). Confirmation of cleavage at Lys^{856} is provided by direct sequence analysis of its 10 N-terminal amino acids (KSSGDGPDLR). In accord with our findings, a thorough analysis of nNOS trypsinolysis, in the absence of bound CaM, indicates that Lys^{856} becomes a cut site following initial cleavage within the CaM binding site at Arg^{727} (32). Since Lys^{856} is protected from tryptic cleavage in the absence of CaM, but exposed when CaM is bound (or the CaM binding site is severed), we conclude that CaM displaces the FMN domain insert peptide of nNOS.

A similar conclusion is drawn from study of eNOS fragmentation after limited trypsinolysis. When CaM is not bound, tryptic cleavage of eNOS yields four principal peptides of nominal molecular masses of 57, 60, 68, and 77 kDa (Fig. 5*B*). This pattern is rationalized by cleavage at Arg^{518} within the CaM

TABLE I
Peptide derivation and composition

Sequence and derivation of polypeptides excerpted from the insert in the FMN binding domain of cNOSs and tested for effects on NOS activity and binding.

Designation	Derivation[a]	Sequence
$eNOS_{628–633}$	b	WRRKRK
$eNOS_{626–636}$	b	SSWRRKRKESS
$nNOS_{835–845}$	h	QEERKSYKVRF
$eNOS_{604–615}$	h	RPEQHKSYKIRF
$eNOS_{601–633}$	b	SSPRPEQHKSYKIRFNSVSCSDPLVSSWRRKRK
$eNOS_{607–634}$	b	QHKSYKIRFNSVSCSDPLVSSWRRKRKE
$nNOS_{851–864}$	r	SDSRKSSGDGPDLR
$nNOS_{835–864}$	h	QEERKSYKVRFNSVSSYSDSQKSSGDGPDL

[a] h, human; b, bovine, r, rat.

TABLE II
The FMN binding domain insert of cNOSs: effect of peptide fragments on NOS activity and ligand binding

Peptide		NOS activity[a]			Ligand Binding to nNOS[b]	
		nNOS	eNOS	iNOS	[^{3}H]-NNA	^{125}I-CaM
	μg/ml (μM)			% of control		
$eNOS_{628–633}$	100 (107.0)	11.0 ± 3.3	24.0 ± 2.8	91.1 ± 5.7	91.7 ± 5.1	6.7 ± 3.6
$eNOS_{626–636}$	100 (71.2)	19.1 ± 0.9	27.7 ± 2.0	92.1 ± 1.3	120.7 ± 12.7	0.0 ± 0.5
$nNOS_{835–845}$	100 (68.1)	102.0 ± 2.1	93.6 ± 2.3	101.1 ± 3.7	118.9 ± 4.1	82.7 ± 1.1
$eNOS_{604–615}$	100 (63.0)	54.5 ± 1.8	80.5 ± 2.0	99.7 ± 5.7	115.0 ± 8.6	24.7 ± 2.2
$eNOS_{601–633}$	300 (76.0)	30.4 ± 1.7	57.2 ± 7.5	62.2 ± 2.8	116.3 ± 1.9	0.0 ± 7.4
$eNOS_{607–634}$	300 (87.7)	28.2 ± 0.9	40.2 ± 4.0	64.3 ± 3.2	122.4 ± 1.0	0.0 ± 4.8
$nNOS_{851–864}$	100 (72.0)	98.4 ± 1.9	102.6 ± 4.1	99.7 ± 2.8	119.2 ± 3.4	89.2 ± 6.2
$nNOS_{835–864}$	300 (84.8)	103.0 ± 1.3	80.2 ± 3.8	84.1 ± 3.5	95.7 ± 4.7	82.7 ± 1.1

[a] NOS activity measurements were performed using purified recombinant nNOS and eNOS, or native iNOS. Values are means ± S.E. of triplicate determinations.

[b] Radioligand binding was performed after incubation of 1–2 pmol of NOS for 15 min at 23 °C with either ^{125}I-calmodulin (1 nM) or [^{3}H]N^G-nitro-L-arginine (NNA) (200 pM) and the indicated peptides. Values are means ± S.E. of triplicate determinations.

The material on this page was copied from the collection of the National Library of Medicine by a third party and may be protected by U.S. Copyright law.

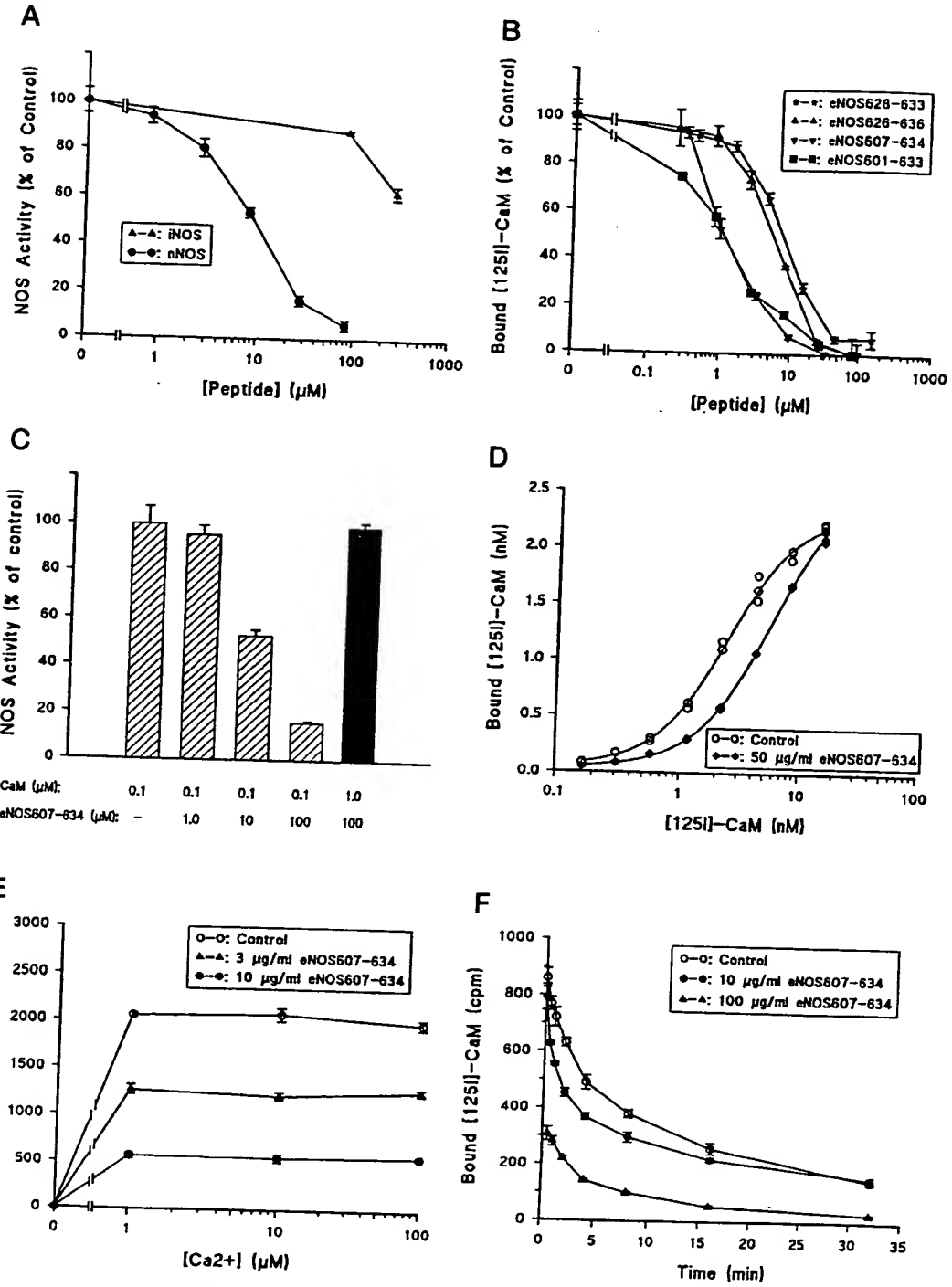

FIG. 3. **Influence of eNOS-insert peptides on NOS activity and CaM binding.** *Panel A*, NOS activity is inhibited by $eNOS^{601-633}$. nNOS activity was measured kinetically, based on the rate of NADPH consumption; iNOS activity was measured as the rate of NO formation, based on Fe^{2+}-myoglobin oxidation. Activities are expressed as percent of control samples in which $eNOS^{601-633}$ was omitted. *Panel B*, ^{125}I-CaM binding to nNOS is inhibited by eNOS insert-derived peptides. Specific inhibition of ^{125}I-CaM binding to nNOS was assessed as a function of concentration of added peptide in a 96-well microfiltration plate assay. *Panel C*, Inhibition of nNOS activity by $eNOS^{607-634}$ is reversed by excess CaM. Activity was measured as percent NADPH consumption rate in the presence of a maximally effective concentration of CaM (0.1 mM), prior to addition of peptide. Note that inhibition of nNOS activity was greater than 80% after addition of 100 mM $eNOS^{607-634}$, but restored to the control level by addition of 10-fold more CaM (*solid bar*). *Panel D*, Inhibition of ^{125}I-CaM binding to nNOS by $eNOS^{607-634}$ is competitive with [CaM]. ^{125}I-CaM binding assays were performed as for *panel B*, over a range of CaM concentrations in the absence (*control*) or presence of peptide. *Panel E*, inhibition of CaM binding to nNOS by $eNOS^{607-634}$ is not reversed by Ca^{2+} excess. ^{125}I-CaM binding assays were performed as for *panel B*, except that $CaCl_2$ concentrations were varied. "Zero" Ca^{2+} (<1 nM) was achieved by inclusion of 10 mM EGTA. *Panel F*, dissociation of ^{125}I-CaM from nNOS is accelerated by $eNOS^{607-634}$.

binding site ($eNOS^{1-518}$ = 56,877 Da, $eNOS^{519-1204}$ = 76,308 Da) and at a second site, likely to be Lys^{545}, which resides between the CaM binding site and insert peptide ($eNOS^{1-545}$ = 59,916; $eNOS^{546-1204}$ = 73,270). Exposure of Lys^{545} and proximity to the CaM binding site is predicted in the model shown in Fig. 2; this site appears to be within a helix-turn transition at the edge of the β-sheet distant from the FMN binding site. Lack of cleavage in nNOS at the site homologous to eNOS Lys^{545} may be explained by the presence of a single basic residue, while eNOS contains paired basic residues (RK). In

The material on this page was copied from the collection of the National Library of Medicine by a third party and may be protected by U.S. Copyright law.

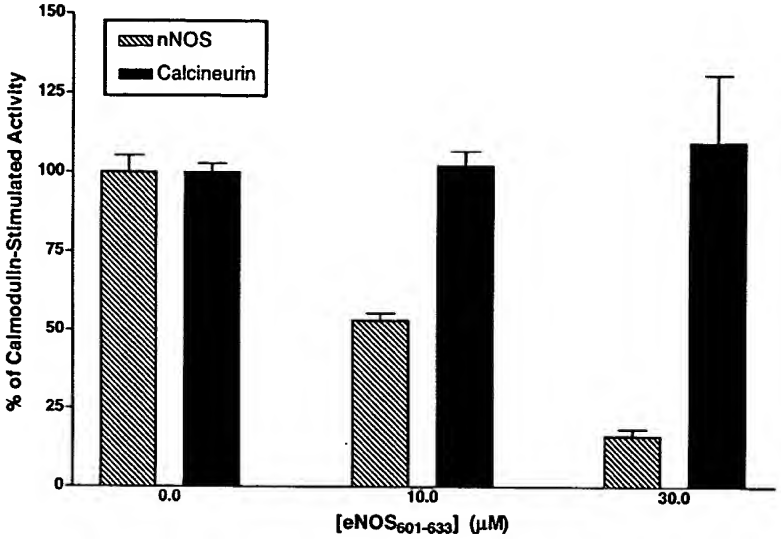

FIG. 4. **CaM-stimulated nNOS activity, but not calcineurin activity, is inhibited by the FMN insert-derived peptide $eNOS_{607-633}$.** Kinetic assays were performed as described under "Experimental Procedures"; *bars* represent means of triplicate determinations ± S.E., performed in the absence and presence of the indicated peptide concentrations. Reaction blanks were performed in the presence of 10 mM EGTA to define CaM-dependent activity of nNOS and calcineurin. In both cases, EGTA reduced activity to a level >10% of that measured in the absence of calcium chelator.

any event, binding of CaM simplifies this cleavage pattern by providing a single dominant cut site. Neglecting the intact proteins and the 10-kDa band from small unresolved fragments of eNOS, only two strong bands are visible at 60 and 65 kDa. These are predicted by cleavage of the molecule within the pentabasic RRKRK motif in the insert peptide at residue Lys^{632}. Thus, cleavage at Lys^{632} (with additional cleavage of the N-terminal fragment at Lys^{545}) produces fragments of 59,916 Da ($eNOS^{1-545}$) and 63,251 Da ($eNOS^{633-1024}$). Alignment reveals close correspondence between Lys^{632} of eNOS and Lys^{856} of nNOS (see Fig. 1), suggesting that CaM binding similarly displaces the insert peptide in each cNOS isoform.

To summarize, CaM binding not only protects the CaM binding site from degradation by trypsin, but exposes cleavage sites on both nNOS and eNOS, which are otherwise inaccessible. A preponderance of evidence points to the clusters of basic residues in the FMN domain insert as the trypsin cleavage sites which are exposed by CaM binding. Exposure of cryptic sites by CaM binding could occur by an allosteric mechanism, or by displacement through binding domain overlap. CaM-driven movement of the insert strongly suggests a switch function for activation of NO synthesis.

Mechanism of NOS Control—Herein we have shown that cNOSs possess a polypeptide insert in their FMN binding modules that is 1) unique to NOS isoforms which are regulated by transient CaM binding; 2) positioned adjacent to the CaM binding domain; 3) an impediment to CaM binding and hence, NOS activation; and 4) displaced when CaM binding *does* occur. Together, these results strongly imply that the insertion in cNOSs is an autoinhibitory control element. We propose that inhibition of NOS by the insert requires occupancy of key sites on cNOS. CaM binding displaces the insert, thus activating cNOS catalysis by "disinhibition." Close proximity of the inhibitory polypeptide to its cognate binding site(s) on cNOSs would result in an exceedingly high local concentration, thus favoring the bound/inhibited state in the absence of CaM. The detection of basal activity with either purified eNOS or nNOS, in the simultaneous presence of EGTA and absence of CaM (≈5% of maximal),[3,4] may arise from a low steady-state concentration of the disinhibited cNOS conformer.

The control mechanism requires that CaM displace the insert upon binding to cNOS; this should translate into a reduced affinity for CaM. Reciprocally, absence of the insert from iNOS would preclude the otherwise expected steric hindrance to CaM binding, contributing to the much tighter binding of CaM at low levels of Ca^{2+}. Studies of polypeptides, corresponding to the putative CaM binding sites on eNOS and iNOS, and of chimeras in which the putative CaM binding sequence of one NOS isoform is substituted with the corresponding portion of another, have indicated that affinity and calcium-dependence of CaM binding is provided by elements on NOS in addition to the recognized CaM binding sequence itself (6, 7). These results have been interpreted as indicating the presence of an auxiliary CaM binding region on iNOS that augments binding. An alternative explanation, raised by our findings, is that the absence of the autoinhibitory polypeptide from iNOS contributes to enhanced CaM affinity at low Ca^{2+} levels. We hypothesize that iNOS evolved from an ancestral cNOS-like protein by loss of the inhibitory peptide; nonetheless, vestigial regulatory sites are suggested by a weak inhibition of activity in the presence of synthetic fragments of the eNOS inhibitory peptide. The CaM binding sites on iNOS and cNOS are apparently related to a similar basic region near the N terminus of CPR, and may have evolved from such a region in a common ancestral protein.

Our data suggest that binding of the inhibitory peptide may involve at least two regions. At least one recognition site binds the RRKRK motif. A second possible site might recognize sequences such as EERKSYKVRF and EQHKSYKIRF that occur in the N-terminal half of the eNOS and nNOS insertions; peptides that lack RRKRK but contain these sequences weakly inhibit NOS activity and CaM binding. Some similarity between the first and second halves of the insertion can be readily noted by comparing the sequences of peptide $eNOS^{628-633}$ and $eNOS^{626-636}$ with those of $nNOS^{835-845}$ and $eNOS^{604-615}$. The insert peptide also contains an abundance of serine and threonine residues which provide potential sites for phosphorylation (12/45 residues in the bovine eNOS insert). We speculate that phosphorylation/dephosphorylation may influence the affinity of insert peptides for binding cognate sites on cNOSs and hence, impact on parameters of NOS activation and/or deactivation. In this regard, it is notable that skeletal muscle possesses an nNOS splice variant in which the insert peptide is expanded by 36 residues (33), providing additional sites for possible cell-type specific modification.

Many important questions remain to be answered. The location and identity of the sites of interaction with the inhibitory polypeptide on the surface of the enzyme are not known. Regions of interaction could include the flanking surface loops of

[3] Q. Liu and S. Gross, unpublished observation.
[4] P. Martasek and B. S. S. Masters, unpublished observation.

The material on this page was copied from the collection of the National Library of Medicine by a third party and may be protected by U.S. Copyright law.

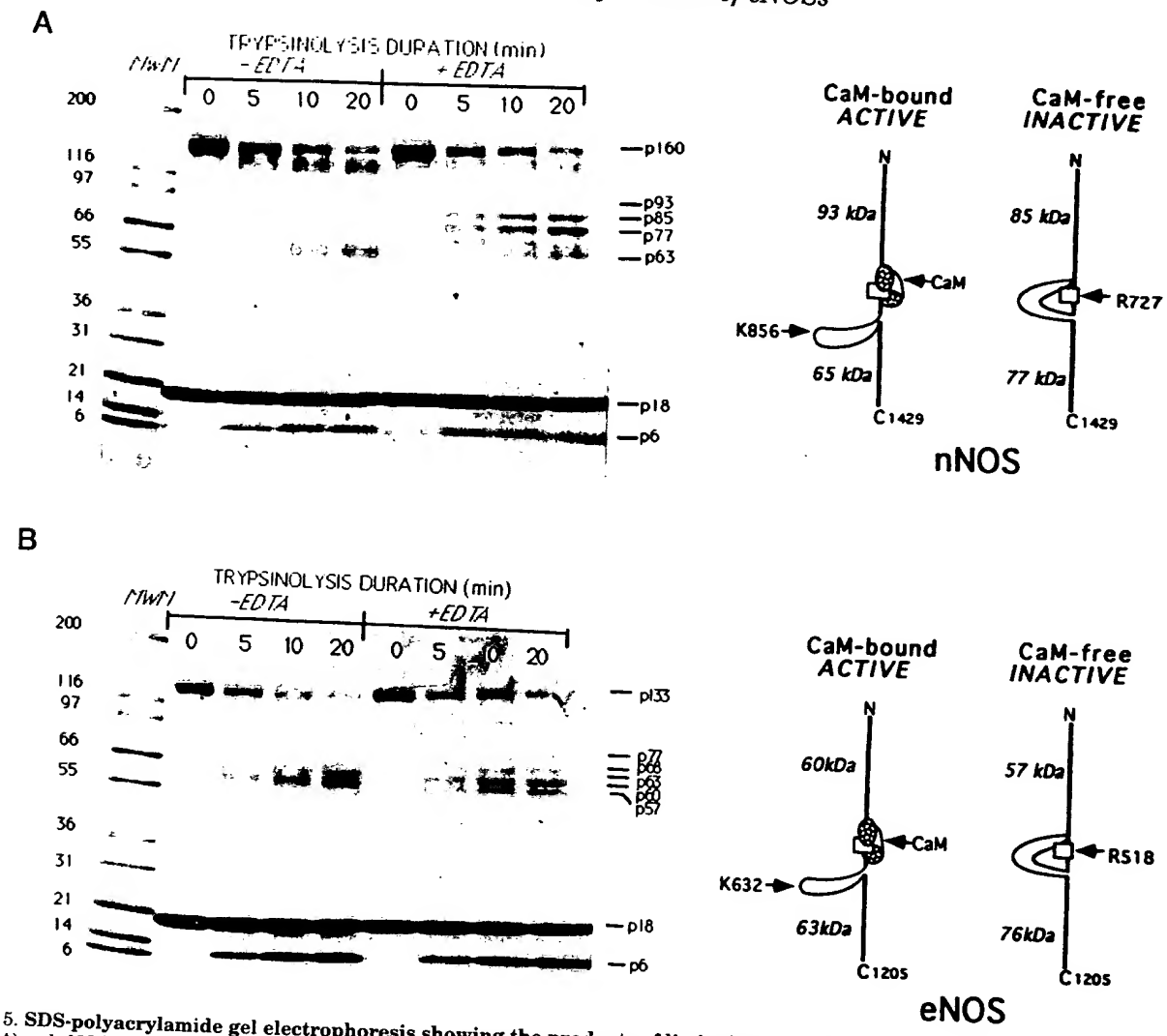

FIG. 5. **SDS-polyacrylamide gel electrophoresis showing the products of limited tryptic digestion of cNOSs.** Trypsinolysis of nNOS (*panel A*) and eNOS (*panel B*) was performed for the indicated duration in the absence (*+EDTA*) or presence (*−EDTA*) of bound CaM. Protein bands at 160, 133, and 17 kDa correspond to uncut nNOS, eNOS, and CaM, respectively. Results indicate that a preferred tryptic cleavage site resides within the CaM binding sequence of cNOSs, however, when this site is masked by bound CaM, a novel tryptic cleavage is revealed within the FMN domain polypeptide insert. *Panel A* shows the progressive formation from nNOS of 75- and 85-kDa fragments in the absence of bound CaM (*lanes 2–5*), and the accumulation of two alternative fragments of 63 and 93 kDa when CaM is bound (*lanes 6–9*). *Panel B* shows the corresponding experiment with eNOS giving a more complicated tryptic cleavage pattern in the absence of bound CaM (*lane 6–9*) that is simplified to two major fragments of 60 and 65 kDa when CaM is bound (*lanes 2–5*). See text for detailed interpretation of cleavage sites.

the FMN domain, bound CaM, and additional more distant sites. In particular, a site on the oxygenase domain consisting of an array of acidic groups could serve as a binding site for the basic regions on the inhibitory polypeptide insert which stabilizes the inhibited conformation of cNOS.

While it seems clear that CaM binding and activation of cNOS is associated with displacement of the inhibitory polypeptide, it is not known how the presence of the polypeptide in its initial conformation inhibits electron transfer. An obvious mechanism would involve interference by the inhibitory polypeptide with interactions between the oxygenase and reductase domains or flavin subdomains, stabilizing a conformation which does not support rapid electron transfer. Such interference could involve changes in either heme/FMN or FMN/FAD distances driven by domain realignment. Intramolecular electron transfer rates are often determined by the ability of electrons to tunnel, and therefore fall off exponentially with distance at roughly an order of magnitude per bond length (34); thus, a small increase in interdomain distance could produce a large reduction in electron flux. Displacement of the inhibitory peptide may not be the only mechanism by which CaM binding stabilizes the activate conformation of cNOSs, inasmuch as CaM removal results in inactivation of iNOS.

In conclusion, we have identified a novel control element in cNOSs which will serve as a prototype for the development of potent peptide inhibitors. The exposure of tryptic cleavage sites in this element represents the first demonstration of a specific CaM-induced conformational change in NOS and may be a hallmark of the active conformer of NOS. Abu-Soud and Stuehr (21) pointed out that the use of CaM to control electron transfer is unique to cNOS. A more fundamental difference between cNOS and other CaM-regulated proteins is the lack of a CaM analog within the cNOS inhibitory peptide. Ultimately, cNOS may not be unique in this regard; it may presage the identification of other CaM regulated systems in which the CaM/inhibitor interaction is mediated through binding domain overlap or allosteric effects, rather than competition for a common recognition site.

Acknowledgments – The encouragement and support of Joe DeAngelo and APEX Biosciences Inc. are responsible for the pilot studies that brought this investigation to fruition.

The material on this page was copied from the collection of the National Library of Medicine by a third party and may be protected by U.S. Copyright law.

REFERENCES

1. Nathan, C., and Xie, Q. W. (1994) *Cell* **78**, 915–918
2. Ignarro, L. J. (1990) *Annu. Rev. Pharmacol. Toxicol.* **30**, 535–560
3. Moncada, S., Palmer, R. M., and Higgs, E. A. (1989) *Biochem. Pharmacol.* **38**, 1709–1715
4. Nathan, C., and Xie, Q. W. (1994) *J. Biol. Chem.* **269**, 13725–13728
5. Cho, H. J., Xie, Q. W., Calaycay, J., Mumford, R. A., Swiderek, K. M., Lee, T. D., and Nathan, C. (1992) *J. Exp. Med.* **176**, 599–604
6. Venema, R. C., Sayegh, H. S., Kent, J. D., and Harrison, D. G. (1996) *J. Biol. Chem.* **271**, 6435–6440
7. Ruan, J., Xie, Q., Hutchinson, N., Cho, H., Wolfe, G. C., and Nathan, C. (1996) *J. Biol. Chem.* **271**, 22679–22686
8. Jarrett, H. W., and Madhavan, R. (1991) *J. Biol. Chem.* **266**, 362–371
9. Brickey, D. A., Bann, J. G., Fong, Y. L., Perrino, L., Brennan, R. G., and Soderling, T. R. (1994) *J. Biol. Chem.* **269**, 29047–29054
10. Dayhoff, M. O., Hunt, W. C., and Hunt, L. T. (1983) *Methods Enzymol.* **91**, 524–545
11. McMillan, K., Bredt, D. S., Hirsch, D. J., Snyder, S. H., Clark, J. E., and Masters, B. S. (1992) *Proc. Natl. Acad. Sci. U. S. A.* **89**, 11141–11145
12. Martasek, P., Liu, Q., Liu, J., Roman, L. J., Gross, S. S., Sessa, W. C., and Masters, B. S. (1996) *Biochem. Biophys. Res. Commun.* **219**, 359–365
13. Gross, S. S., and Levi, R. (1992) *J. Biol. Chem.* **267**, 25722–25729
14. Gross, S. S. (1996) *Methods Enzymol.* **268**, 159–168
15. Bolton, A. E., and Hunter, W. M. (1973) *Biochem. J.* **133**, 529–539
16. Nishimura, J. S., Martasek, P., McMillan, K., Salerno, J., Liu, Q., Gross, S. S., and Masters, B. S. (1995) *Biochem. Biophys. Res. Commun.* **210**, 288–294
17. Takai, A., and Mieskes, G. (1991) *Biochem. J.* **275**, 233–239
18. Masters, B. S., McMillan, K., Sheta, E. A., Nishimura, J. S., Roman, L. J., and Martasek, P. (1996) *FASEB J.* **10**, 552–558
19. Liu, Q., and Gross, S. S. (1996) *Methods Enzymol.* **268**, 311–324
20. Sheta, E. A., McMillan, K., and Masters, B. S. (1994) *J. Biol. Chem.* **269**, 15147–15153
21. Abu-Soud, H. M., and Stuehr, D. J. (1993) *Proc. Natl. Acad. Sci. U. S. A.* **90**, 10769–10772
22. Bredt, D. S., Hwang, P. M., Glatt, C. E., Lowenstein, C., Reed, R. R., and Snyder, S. H. (1991) *Nature* **351**, 714–718
23. Porter, T. D. (1991) *Trends Biochem. Sci.* **16**, 154–158
24. Watenpaugh, K. D., Sieker, L. C., and Jensen, L. H. (1973) *Proc. Natl. Acad. Sci. U. S. A.* **70**, 3857–3860
25. Yuda, M. (1996) GenBank™ accession no. U59389
26. Regulski, M., and Tully, T. (1995) *Proc. Natl. Acad. Sci. U. S. A.* **92**, 9072–9076
27. Kim, J.-J., Wang, M., Roberts, D. L., Paschke, R., Shea, T., and Masters, B. S. S. (1996) in *Flavins and Flavoproteins* (Stevenson, K. J., ed) pp. 455–462, University of Calgary Press, Calgary, Alberta, Canada
28. Rossmann, M. G., Moras, D., and Olsen, K. W. (1974) *Nature* **250**, 194–199
29. O'Neil, K. T., and De Grado, W. F. (1990) *Trends Biochem. Sci.* **15**, 59–64
30. Vorherr, T., Knopfel, L., Hofmann, F., Mollner, S., Pfeuffer, T., and Carafoli, E. (1993) *Biochemistry* **32**, 6081–6088
31. Imparl, J. M., Senshu, T., and Graves, D. J. (1995) *Arch. Biochem. Biophys.* **318**, 370–377
32. Lowe, P. N., Smith, D., Stammers, D. K., Riveros-Moreno, V., Moncada, S., Charles, I., and Boyhan, A. (1996) *Biochem. J.* **314**, 55–62
33. Silvagno, F., Xia, H., and Bredt, D. S. (1996) *J. Biol. Chem.* **271**, 11204–11208
34. Moser, C. C., Keske, J. M., Warncke, K., Farid, R. S., and Dutton, P. L. (1992) *Nature* **355**, 796–802

The material on this page was copied from the collection of the National Library of Medicine by a third party and may be protected by U.S. Copyright law.

Proc. Natl. Acad. Sci. USA
Vol. 92, pp. 8428–8432, August 1995
Biochemistry

EXHIBIT B

High-level expression of functional rat neuronal nitric oxide synthase in *Escherichia coli*

LINDA J. ROMAN*, ESSAM A. SHETA*†, PAVEL MARTASEK*, STEVEN S. GROSS‡, QING LIU‡, AND BETTIE SUE SILER MASTERS*§

*Department of Biochemistry, The University of Texas Health Science Center, San Antonio, TX 78284-7760; and ‡Department of Pharmacology, Cornell University Medical College, New York, NY 10021

Communicated by Ronald W. Estabrook, The University of Texas Southwestern Medical Center, Dallas, TX, June 1, 1995 (received for review April 10, 1995)

ABSTRACT **The neuronal nitric oxide synthase (nNOS) has been successfully overexpressed in *Escherichia coli*, with average yields of 125–150 nmol (20–24 mg) of enzyme per liter of cells. The cDNA for nNOS was subcloned into the pCW vector under the control of the *tac* promotor and was coexpressed with the chaperonins groEL and groES in the protease-deficient BL21 strain of *E. coli*. The enzyme produced is replete with heme and flavins and, after overnight incubation with tetrahydrobiopterin, contains 0.7 pmol of tetrahydrobiopterin per pmol of nNOS. nNOS is isolated as a predominantly high-spin heme protein and demonstrates spectral properties that are identical to those of nNOS isolated from stably transfected human kidney 293 cells. It binds N^{ω}-nitroarginine dependent on the presence of bound tetrahydrobiopterin and exhibits a K_d of 45 nM. The enzyme is completely functional; the specific activity is 450 nmol/min per mg. This overexpression system will be extremely useful for rapid, inexpensive preparation of large amounts of active nNOS for use in mechanistic and structure/function studies, as well as for drug design and development.**

Nitric oxide synthase (NOS) catalyzes the formation of NO· and L-citrulline from L-arginine through a series of oxidations using molecular oxygen (1). There are three separate genes known to encode the NOS family of proteins, including the constitutively expressed neuronal (nNOS) (2) and endothelial cell (ecNOS) (3, 4) isoforms and the inducible isoform (iNOS) (5, 6). The product of the NADPH-mediated reaction, NO·, has been implicated in neurotransmission in the brain and in neuromuscular junctions (nNOS), hemodynamic regulation (ecNOS), and cytotoxicity (iNOS). The effects of NO· produced by the nNOS and ecNOS are thought to be mediated through stimulation of guanylate cyclase activity, whereas the NO· produced by iNOS appears to act directly or via peroxynitrite on foreign cells (for reviews, see refs. 7 and 8).

The three isoforms differ in primary sequence, having only 50–60% sequence identity (9), size, intracellular location, and regulation. nNOS (160 kDa) and iNOS (130 kDa) were purified from the cytosol (8, 10–12), whereas the ecNOS (135 kDa) was found to be membrane-bound (13). The nNOS and ecNOS are constitutively expressed but modulated by intracellular Ca^{2+} levels (1, 14), unlike iNOS, which is induced by bacterial endotoxin and is Ca^{2+}-independent (15). All three isoforms bind calmodulin and tetrahydrobiopterin (BH_4), as well as molar ratios of heme, FMN, and FAD (11–13, 16–20). These members of the NOS family are the only mammalian enzymes that catalyze both hydroxylation and NADPH reduction of flavins within the same protein, an attribute shared only by the *Bacillus megaterium* enzyme, cytochrome $P450_{BM-3}$ (21).

Mechanistic and structure/function studies of nNOS had initially been very difficult due to the minute amounts of protein that can be purified from cerebellar tissue. Bredt and Snyder (1), who initially isolated nNOS, reported a yield of 9 μg of pure protein from 18 rat brains. Bredt *et al.* (2) subsequently cloned and expressed nNOS in human kidney 293 cells, providing a 10-fold enrichment of nNOS in cultured cells over rat brain. Twelve liters of these cultured cells consistently yield 8–10 mg of nNOS (K. McMillan and B.S.S.M., unpublished observation). Although this is a significant improvement over initial yields, the expense and time involved in mammalian cell culture are extensive. Other laboratories have expressed nNOS using baculovirus overexpression systems. Charles *et al.* (22) report successful expression, but the majority of their recombinant nNOS is insoluble and inactive; the recombinant enzyme has a specific activity that is 100-fold lower than that of native nNOS isolated from rat cerebellar tissue. Richards and Marletta (23) improved the yield of active enzyme from the baculovirus system by adding hemin to the medium but still can isolate only ≈1 mg of pure protein from 7–10 75-cm^2 monolayer cultures, only about half of which contains heme.

In this paper, we report the overexpression of active nNOS in *Escherichia coli*. Expression was directed under the *tac* promoter of the pCW_{ori+} vector, a system that has been instrumental in the expression of cytochromes P450 (24, 25). This vector was chosen to promote the proper insertion of heme, as occurs for *E. coli*-expressed cytochromes P450, in an effort to abate a major drawback of the baculoviral system, poor heme incorporation. Because initial experiments were plagued by highly proteolyzed and dysfunctional protein, an expression plasmid for the chaperonins groEL and groES (26) was also included.

MATERIALS AND METHODS

Chemicals. L-[2,3-^{3}H]Arginine was obtained from DuPont/NEN, and BH_4 was from Research Biochemicals (Natick, MA). All other chemicals were obtained from Sigma and were of the highest grade available.

Enzymes. *Taq* polymerase, ligase, and restriction enzymes were purchased from either Promega or New England Biolabs. Shrimp alkaline phosphatase was from United States Biochemical.

Plasmids. pNOS (2), containing the rat nNOS cDNA in pBluescript SK(−), was provided by Solomon Snyder and David Bredt at Johns Hopkins Medical School, Baltimore. pGroESL (27), containing groEL and groES cDNAs, was from

The publication costs of this article were defrayed in part by page charge payment. This article must therefore be hereby marked "*advertisement*" in accordance with 18 U.S.C. §1734 solely to indicate this fact.

Abbreviations: NOS, nitric oxide synthase; nNOS, neuronal isoform of NOS; ecNOS, endothelial cell isoform of NOS; iNOS, inducible macrophage isoform of NOS; BH_4, tetrahydrobiopterin; NNA, N^{ω}-nitro-L-arginine; NMA, *N*-methyl-L-arginine.

†Present address: Department of Biochemistry, Alexandria University, Alexandria, Egypt.
§To whom reprint requests should be addressed.

The material on this page was copied from the collection of the National Library of Medicine by a third party and may be protected by U.S. Copyright law.

Paul Horowitz at The University of Texas Health Science Center at San Antonio. pCW_{ori+} (28) was provided by Michael Waterman at Vanderbilt University, Nashville, TN.

Recombinant DNA Manipulations. nNOSpCW, the plasmid for the expression of nNOS in *E. coli*, was constructed as follows. The initial 1210 nt of pNOS (from the ATG start codon to the *Nar* I restriction site) were amplified by PCR to incorporate the recognition sequence for *Nde* I. Primer 1 (upstream primer, with *Nde* I site) was 5′-TCATCATCAT-ATGGCTGAAGAGAACACGTT-3′, and primer 2 (return primer) was 5′-CATGCTTGGCGCCAT-3′. Primers were synthesized by the Center for Advanced DNA Technologies at The University of Texas Health Science Center at San Antonio. Reaction mixtures included 50 pmol of each primer, 20 ng of pNOS template, 200 μM dNTPs, 1.5 mM $MgCl_2$, 1× *Taq* polymerase buffer (50 mM KCl/10 mM Tris·HCl, pH 9.0/0.1% Triton X-100), and 2.5 units of *Taq* polymerase in 100-μl total volume. The mixture was preincubated for 3 min at 94°C before the addition of *Taq* polymerase, followed by amplification for 30 cycles: 94°C for 30 s, 55°C for 60 s, and 72°C for 90 s. The PCR product was gel-purified using the GeneClean II kit (Bio 101) and digested with *Nde* I and *Nar* I. pNOS DNA was then restricted with *Nar* I and *Xba* I to generate the remaining 3529 nt of the NOS cDNA sequence, which was also gel-purified. pCW_{ori+} DNA was digested with *Nde* I and *Xba* I, and the ends were dephosphorylated. The three pieces were ligated, and the resultant products were used to transform *E. coli*. JM109 competent cells were purchased from Stratagene and transformed by using the manufacturer's instructions.

The transformation mixture was plated on LB agar containing ampicillin at 50 μg/ml, and nine colonies were screened by *Bam*HI restriction digest of alkaline lysis plasmid minipreparations. Five positive clones were further screened for isopropyl β-D-thiogalactoside-induced (0.5 mM, added at OD_{600} = 0.8, along with 225 μM δ-aminolevulinic acid) expression of nNOS at 37°C by immunoblot analysis of whole cells using rabbit anti-rat nNOS IgG. All five clones exhibited bands that comigrated with that of nNOS isolated from kidney 293 cells.

In subsequent manipulations, when pGroELS was cotransformed with nNOSpCW, transformants were plated on LB agar containing ampicillin at 50 μg/ml and chloramphenicol at 35 μg/ml. Due to severe proteolysis of nNOS when JM109 cells were lysed, both plasmids were also cotransformed into the protease-deficient *E. coli* strain BL21. Transformation of BL21 was via electroporation using an Invitrogen electroporator II according to manufacturer's instructions.

Protein Expression. Fernbach flasks containing 1 liter of modified Terrific Broth (20 g of yeast extract, 10 g of bactotryptone, 2.65 g of KH_2PO_4, 4.33 g of Na_2HPO_4, and 4 ml of glycerol) and ampicillin at 50 μg/ml and, when pGroELS was present, chloramphenicol at 35 μg/ml were inoculated with 1 ml of an overnight culture (grown in LB plus antibiotics) and shaken at 250 rpm at 37°C. Protein expression was induced at OD_{600} = 1.0–1.4 with the addition of isopropyl β-D-thiogalactoside to 0.5 mM. The heme and flavin precursors, δ-aminolevulinic acid and riboflavin, were also added to final concentrations of 450 μM and 3 μM, respectively. When pGroELS was present, the culture medium also contained 1 mM ATP. The flasks were moved to room temperature (25°C) and shaken in the dark at 250 rpm. The cells were harvested at ≈40 hr after induction, and the cell paste was frozen at −80°C until purification.

JM109 cells containing pNOSpCW grown after induction at 37°C exhibit no detectable peak at 445 nm in CO difference spectra; all protein is present as a 420-nm species. JM109 cells containing pNOSpCW grown at 25°C for 36–40 hr after induction have both 445- and 420-nm species; this protein is heavily proteolyzed upon cell lysis, as judged by immunoblot analysis. The absolute amount of protein production in JM109 cells is enhanced 5- to 10-fold upon coexpression of nNOS with groEL and groES, but this protein is still heavily proteolyzed upon cell lysis. A small amount of activity (1% that of nNOS purified from 293 cells, data not shown) can be detected. BL21 cells containing pNOSpCW do not appear to express nNOS as detectable by CO difference spectra. BL21 cells containing both pNOSpCW and pGroELS, however, produce 125–150 nmol of nNOS (20–24 mg) per liter of culture, as quantitated by CO difference spectra. All data presented in this paper are derived using protein purified from BL21 that has been cotransformed with both pNOSpCW and pGroELS.

Protein Purification. Harvested cells were resuspended in 30 ml of resuspension buffer (100 mM Tris·HCl, pH 7.4/1 mM EDTA/1 mM dithiothreitol/10% (vol/vol) glycerol/1 mM phenylmethylsulfonyl fluoride/leupeptin at 5 μg/ml/pepstatin at 5 μg/ml per liter of initial culture and were lysed by pulsed sonication (4 min, 80% power, large probe, Fisher Scientific model 550). Cell debris was removed by centrifugation at 150,000 × *g* for 70 min. The supernatant was applied to a 2′,5′-ADP-Sepharose 4B column (6 ml, Pharmacia) equilibrated in buffer B (50 mM Tris·HCl, pH 7.4/0.1 mM EDTA/0.1 mM dithiothreitol/10% glycerol/100 mM NaCl). The column was extensively washed with at least 10 column volumes of buffer B and then washed again with buffer B/500 mM NaCl. The protein was eluted with buffer B/500 mM NaCl/5 mM 2′-AMP. The colored fractions were pooled and concentrated (Centriprep 30, Amicon), and L-arginine and BH_4 were added to final concentrations of 2 mM and 1 mM, respectively. This fraction was incubated overnight at 4°C and applied to a S-200 gel filtration column (480 ml, 2.5-cm diameter, Pharmacia) equilibrated in buffer B. The nNOS-containing fractions were pooled, concentrated, and stored at −80°C. All manipulations were done at 4°C. The cytosolic extract contains 125–150 nmol of nNOS (100% yield), as determined by CO difference spectra, the 2′,5′-ADP-Sepharose 4B column pool contains 50–100 nmol of enzyme (≈55% yield), and the S-200 column pool contains 25–45 nmol of enzyme (≈30%). Enzymatic activity, as measured by the conversion of L-arginine to L-citrulline (see below), parallels the heme content. Optimization of this purification procedure may further increase these yields. The ratio of heme to FMN content was determined to be 1:1. The concentrations of the flavins were determined by using the method of Faeder and Siegel (29).

Although a similar procedure used to isolate nNOS from kidney 293 cells yields enzyme that is ≥90% pure, the enzyme isolated from *E. coli* is ≈70% pure, with only one other major contaminant (Fig. 1, lane 5) which, based on immunoblot analysis, is not a proteolytic fragment of nNOS. The spectra and activities presented in this paper were generated using this preparation of enzyme. If, instead of the S-200 gel filtration column, the enzyme is applied to a Mono Q ion-exchange fast protein liquid chromatography column (Pharmacia) in buffer

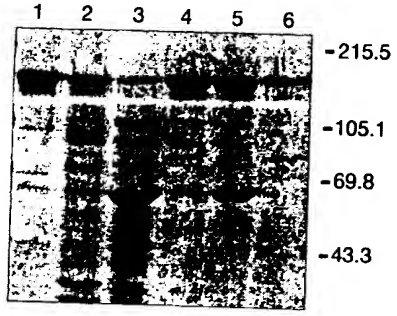

FIG. 1. SDS/PAGE analysis of nNOS during purification. A Coomassie G-250-stained 7.5% polyacrylamide gel is shown. Lanes: 1, 3.5 ng of human kidney 293 cell-expressed nNOS; 2, 15 ng of resuspended membrane fraction; 3, 25 ng of cytosolic extract; 4, 5 ng of 2′,5′-ADP-Sepharose fraction; 5, 5 ng of S-200 column fraction; and 6, 2.5 ng of Mono Q column fraction.

The material on this page was copied from the collection of the National Library of Medicine by a third party and may be protected by U.S. Copyright law.

B and eluted at ≈200 mM NaCl in a 0–500 mM NaCl gradient, this major contaminant is eliminated (Fig. 1, lane 6).

Spectrophotometric Methods. Absolute spectra and CO difference spectra were done essentially as described by McMillan and Masters (30) except that all measurements were done in buffer B, and the CO difference spectra were obtained by reducing the protein and then bubbling the sample cuvette with CO. Substrate perturbation difference spectra were done as described (30), but in the presence of 1 mM imidazole to shift the entire population of nNOS to the low-spin heme state. The molar protein concentration was determined based on heme content and $\Delta\varepsilon_{444-475} = 75\ mM^{-1}$ (18, 31). All spectral analyses were performed by using a Shimadzu model 2101 UV/visible dual-beam spectrophotometer.

Measurement of NO· Formation. Nitric oxide formation was measured by using both the hemoglobin capture assay (32), done at 25°C as described by Sheta *et al.* (33) and the method of Bredt and Snyder (1), which monitors the formation of L-[^{3}H]citrulline from L-[^{3}H]arginine, as described (19). Each reaction mixture, containing 0.5 μg of enzyme, was incubated at 25°C for 2 min (over which time the reaction is linear). For K_m analysis, the concentration of L-[^{3}H]arginine in the reaction mixture was varied over the range of 2.0–10.0 μM.

Pterin Analysis. Determination of pterin content was done as described by Gross and Levi (34), based on the method of Fukushima and Nixon (35), by acid hydrolysis of a 10-ng protein sample followed by quantitation of pterin by C_{18} reverse-phase HPLC.

Determination of N^{ω}-nitro-L-arginine (NNA)-Binding Constant. The NNA-binding constant was determined by direct titration of purified nNOS with [^{3}H]NNA. In these experiments, done in 96-well poly(vinylidene difluoride) plates in 100-μl total volume, 10 pmol of nNOS and radiolabeled NNA (specific activity ≈23,000 dpm/pmol) were incubated at room temperature for 15 min in 50 mM Tris·HCl, pH 7.6/1 mM dithiothreitol, in the presence or absence of 10 μM BH_4. Assays were also done in the presence or absence of 100 μM *N*-methyl-L-arginine (NMA), a potent inhibitor of L-arginine binding. The incubation was stopped by aspiration of the sample through the poly(vinylidene difluoride) membrane. The wells were washed twice with 200 μl of 50 mM Tris, pH 7.6, and air-dried for 10 min; 25 μl of scintillation cocktail was added, and radioactivity of samples was counted.

Determination of Heme Content. The heme content of the purified protein preparation was measured by CO difference spectra (described above) and by the pyridine hemochromogen method (36). A 30-μl aliquot of pyridine was added to 70 μl of purified protein, along with 1.5 μl of 10 M NaOH. The sample was reduced with two grains of dithionite, and the spectrum was read after 2 min. Heme concentration was determined by the absorbance at 556 nm, assuming $\varepsilon = 34\ mM^{-1}$.

RESULTS

Spectral Characteristics of Purified *E. coli*-Expressed Enzyme. Fig. 2 shows the absolute spectrum of nNOS isolated from *E. coli*. It exhibits a broad peak at 400 nm and secondary maxima at 550 and 650 nm, indicative of a predominantly high-spin heme, although some low-spin form is present, as evidenced by the shoulder at 410 nm. Shoulders are also apparent at 450 and 475 nm and are due to flavin absorbance; this spectrum is identical to that of nNOS isolated from human kidney 293 cells (19). As shown in Fig. 2, the maximum heme absorbance at 400 nm can be shifted to the low-spin form (peak at 428 nm) by the addition of imidazole to 1 mM or completely to the high-spin form (peak at 395 nm) by the addition of arginine to 2 μM.

Fig. 2 *Inset* also shows the characteristic cytochrome P450-like CO difference spectrum of nNOS with a peak at 444 nm. The molar concentration of heme-containing enzyme, calculated from the peak at 444 nm, assuming $\Delta\varepsilon_{444-475} = 75\ mM^{-1}$, is 1.9 μM. For comparison, a pyridine hemochromogen was also done to determine the heme concentration (data not shown); this method yielded a concentration of 2.1 μM, in reasonable agreement with that calculated from the CO difference spectrum.

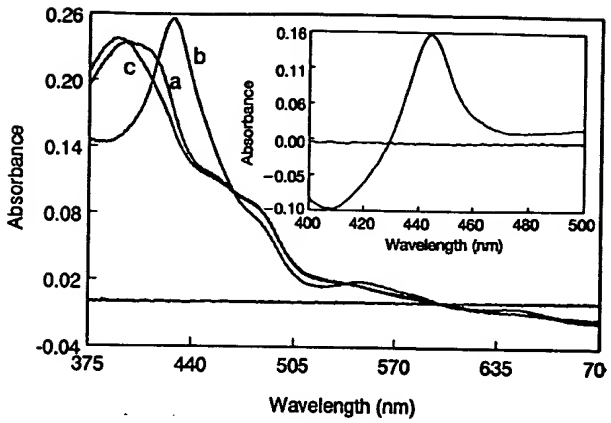

FIG. 2. Absolute absorbance and CO difference spectra of nNOS as purified from *E. coli*. Experiments were done as described using 3.2 μM nNOS. Curve: a, unperturbed spectrum of purified nNOS; b, spectrum after addition of 1 mM imidazole to nNOS; and c, spectrum after addition of 2 μM L-arginine to nNOS. (*Inset*) CO difference spectra, using 1.9 μM nNOS.

With the technique of difference spectrophotometry, the perturbation of the heme spectrum by increments of L-arginine, in the presence of 1 mM imidazole, was measured (Fig. 3). A type I spectrum, characterized by a maximum at ≈390 nm and a minimum at ≈430 nm, was observed. A spectral binding constant (K_s) was calculated from the apparent K_s, derived from a plot of 1/absorbance change vs. 1/[L-arginine] (Fig. 3 *Inset*), using the following equation:

$$\text{apparent } K_s = K_s(1 + [\text{imidazole}]/K_{d\ \text{imidazole}}).$$

Assuming $K_{d\ \text{imidazole}}$ to be 160 μM (30, 37), the value of K_s for arginine binding to nNOS is 717 nM.

Pterin Analysis of Purified *E. coli*-Expressed Enzyme. Pterin content was determined in two different samples of nNOS: (*i*) partially purified enzyme before BH_4 incubation (fraction 1; pre-S-200 column chromatography); (*ii*) purified enzyme after BH_4 incubation (fraction 2; post-S-200 column chromatography). The analysis reveals that, as isolated, fraction

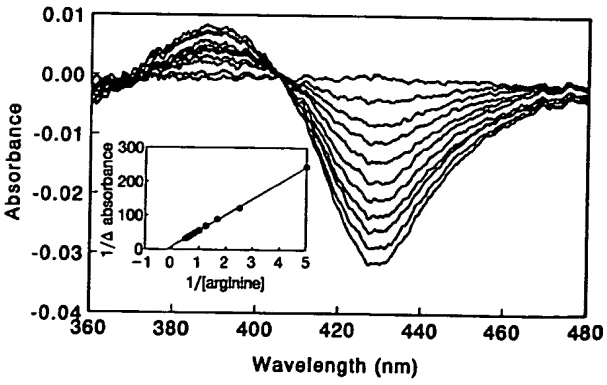

FIG. 3. Substrate perturbation difference spectra of *E. coli*-expressed nNOS. Experiments were done as described by using 1.5 μM nNOS in the presence of 1 mM imidazole. Purified enzyme was titrated with L-arginine to final concentrations of 0, 0.2, 0.4, 0.6, 0.8, 1.0, 1.2, 1.4, 1.6, 1.8, and 2.0 μM (baseline and sequential minima, respectively). (*Inset*) Plot from which the apparent K_s is derived.

The material on this page was copied from the collection of the National Library of Medicine by a third party and may be protected by U.S. Copyright law.

1 contains 0.096 pmol of BH_4 per pmol of nNOS—i.e., 10% of the expressed nNOS contains BH_4 (data not shown). No other pterin moiety was present. This is in contrast to the nNOS heme domain expressed in *E. coli* JM109, which contained only 1–2% BH_4, as well as being ≈30% saturated with non-BH_4 pterin (K. McMillan, S.S.G., and B.S.S.M., unpublished observation). Fraction 2 was complemented with 0.636 pmol of BH_4 per pmol of nNOS—i.e., 64% saturated (data not shown). Thus, if stoichiometric binding of BH_4 is required for activity, this preparation of nNOS contains 64% active enzyme.

Binding of NNA to Purified *E. coli*-Expressed Enzyme. The binding of [^{3}H]NNA as a function of ligand concentration was determined in the presence and absence of additional BH_4 for both fractions 1 (pre-BH_4) and 2 (post-BH_4). Fig. 4 shows that NNA binds significantly to *E. coli*-expressed nNOS fraction 1 (circles) only in the presence of added BH_4. The binding constant (K_d) and the maximum amount of NNA bound (B_{max}) differ greatly depending on whether or not BH_4 is added (*Inset*). Fraction 2 (triangles), which is 65% BH_4-saturated, binds NNA equally well in the presence or absence of added BH_4; K_d and B_{max} are the same, regardless of whether BH_4 is added or not. In the presence of 100 μM *N*-methyl-L-arginine (L-NMA), binding of NNA is essentially abolished in either fraction (data not shown). Thus, NNA binding depends on the presence of bound BH_4 and the K_d for NNA binding is ≈45 nM. In addition, fraction 1 enzyme can be reconstituted with BH_4 up to 54%, and fraction 2 enzyme does not bind additional BH_4—i.e., it appears to be maximally complemented.

Enzymatic Activity of Purified *E. coli*-Expressed Enzyme. The conversion of L-arginine to L-citrulline was assayed for fractions 1 (pre-BH_4) and 2 (post-BH_4) in the presence and absence of additional BH_4. The turnover numbers for fraction 1 were 75 and 202 nmol/min per mg without and with BH_4 in the assay mixture, respectively, a stimulation of 2.7-fold. The turnover numbers for fraction 2 were 189 and 435 nmol/min per mg without and with BH_4 in the assay mixture, respectively, a stimulation of 2.3-fold. The enzymatic activity is inhibited by 95% by 100 μM NMA in all cases; this is consistent with the inhibition of NNA binding by NMA. The turnover numbers for both fractions in the presence of BH_4 were confirmed by using the hemoglobin capture assay; the activities of fractions 1 and 2 were 239 and 468 nmol/min per mg, respectively, demonstrating excellent agreement between the two methods. These turnover numbers are very similar to those obtained with nNOS purified from human kidney 293 cells in which activities between 300 and 450 nmol/min per mg are typically observed.

The K_m value for L-arginine was determined to be 2.8 μM for *E. coli*-purified nNOS (data not shown). Concomitant measurement using human kidney 293 cell-purified nNOS yielded a K_m value of 1.9 μM. These values are in excellent agreement with each other and with the K_m value of 2 μM for nNOS reported by Bredt and Snyder (1) and McMillan *et al.* (19).

DISCUSSION

We have developed a method for the overexpression of nNOS in *E. coli*, a system that offers a quick and inexpensive way to produce large quantities of active enzyme. We can produce 125–150 nmol (20–24 mg) of nNOS per liter of *E. coli* culture. The three elements composing this successful method are the vector used (pCW), the coexpression of chaperonins with nNOS, and the *E. coli* strain in which the proteins are expressed (BL21). It is intriguing that a simple prokaryotic system such as *E. coli* has the ability to overexpress as complex a mammalian enzyme as nNOS, which contains protoporphyrin IX heme, FAD, FMN, and BH_4 as prosthetic groups. The lack of calmodulin produced in this system is an advantage in that the nNOS is not activated to produce cytotoxic NO·.

The production of nNOS is controlled by the *tac* promoter of pCW, an expression vector chosen because it has proved to be invaluable for the expression of cytochromes P450 (24, 25), a family of enzymes to which the N-terminal domain of nNOS has been compared, as well as cytochrome P450/NADPH-cytochrome P450 reductase fusion proteins (38, 39), chimeric constructs that mimic the activities of hydroxylase and reductase domains in a single protein. The heme moiety appears to be inserted correctly into the majority of expressed nNOS protein, as judged by the absolute and CO difference spectra and the spectral perturbation by the substrate L-arginine. The lack of heme repletion, which seems to be a major drawback of the expression of NOS in a baculovirus system (22, 23), is overcome by expression in *E. coli*.

In the current report, nNOS is coexpressed with the *E. coli* groE molecular chaperonin system (groEL and groES). In the absence of these proteins, expression of nNOS is much lower in *E. coli* strain JM109 and undetectable in *E. coli* BL21. Chaperonins facilitate the proper folding of some proteins, probably by inhibiting aggregation and/or by alleviating kinetic blocks to folding, and have made possible the expression

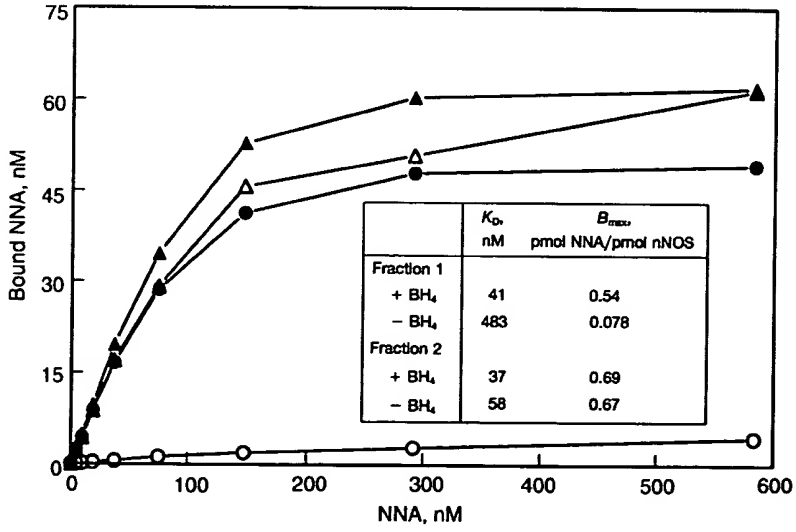

FIG. 4. Binding of [^{3}H]NNA to *E. coli*-expressed nNOS. Experiments were done as described using 10 pmol of nNOS. ○ and ●, Semipurified *E. coli*-expressed nNOS that has been passed over the 2′,5′-ADP-Sepharose 4B column but has not yet been incubated with BH_4 during purification (fraction 1); △ and ▲, purified *E. coli*-expressed nNOS that had been incubated with BH_4 during purification as described (fraction 2); ○ and △, assays done in the absence of additional BH_4; ● and ▲, assays done in the presence of 10 μM BH_4. (*Inset*) Table of binding data described by curves.

The material on this page was copied from the collection of the National Library of Medicine by a third party and may be protected by U.S. Copyright law.

of several mammalian proteins in *E. coli* that did not express otherwise (26, 40). The observation that substantially more nNOS is produced in the presence of chaperonins further demonstrates the usefulness of this approach.

E. coli strain JM109 was initially chosen for the expression of nNOS but, upon lysis of the cells, the calmodulin-binding site proved extremely susceptible to proteolytic attack. As a result of this sensitivity, large amounts of the proteolytically produced domains of *E. coli*-expressed nNOS were initially purified, a problem that was alleviated by coexpressing the nNOS and chaperonins in BL21, a strain reported to be lacking both *lon* and *ompT* proteases.

The nNOS enzyme produced by *E. coli* appears indistinguishable, in all respects examined, from that produced by nNOS stably transfected human kidney 293 cells; the absolute spectrum and its perturbation by the substrate L-arginine (spectral binding constant ≈717 nM), the CO difference spectrum, and the specific activity of *E. coli*-expressed nNOS and mammalian cell-expressed nNOS are identical. The binding of [^{3}H]NNA by nNOS depends on the presence of BH_4, exhibits a binding constant of ≈45 nM, and saturates at ≈1 nmol of [^{3}H]NNA/1 nmol of enzyme. Klatt *et al.* (41) report a K_d of 170 nM for [^{3}H]NNA binding to nNOS and indicate that binding was not dependent on BH_4. This small difference in K_d values may depend on the specific assay used or the degree of BH_4 repletion, although the enzyme used by Klatt *et al.* appears to be BH_4-replete based on their observation that the addition of BH_4 had no effect on [^{3}H]NNA binding.

The *E. coli*-expressed nNOS is extremely active, with a turnover of 450 nmol/min per mg of NOS, as measured by both the hemoglobin capture assay and the conversion of L-[^{3}H]arginine to L-[^{3}H]citrulline, and this activity is 95% inhibited by 100 μM NMA, indicating that NMA is effectively competing at the substrate-binding site. The K_m value of the enzyme for L-arginine is 2.8 μM, in good agreement with both that of nNOS isolated from transfected human kidney 293 cells (≈2 μM) (19) and that reported by Bredt and Snyder (1) for nNOS isolated from rat brain (≈2 μM).

The observation that fraction 2 seems to be fully complemented with BH_4 and yet BH_4 added to the assay increases activity significantly is interesting; perhaps the BH_4 bound to the enzyme is unstable or destroyed during catalysis. The difference between the activities exhibited by the pre- and post-BH_4 fractions, however, is 2-fold whether or not BH_4 is included in the assay; it appears that the earlier the nNOS is saturated with BH_4, the higher the activity—i.e., the more stable the enzyme.

The large amounts of intact, active nNOS, which has a specific activity at least as high as that of kidney 293 cell-expressed enzyme, that can be generated using this system will make possible mechanistic, kinetic, and spectroscopic studies leading to the understanding of structure/function relationships. The approach outlined here may also be useful for the overexpression of the other NOS isoforms, ecNOS and iNOS, in *E. coli*. This overexpression system also provides a source of nNOS that is essentially BH_4-free for analysis of BH_4 function in NOS catalysis. The availability of this quantity of the NOS enzyme will be extremely useful for site-directed mutagenesis and, given the important physiological roles played by the NOS isoforms, drug design and development.

We thank Kirk McMillan and Tim McCabe for advice, helpful discussions, and rabbit antibody to nNOS and Ramani Narayanasami for his aid in the flavin determinations. This work was supported, in part, by Grant AQ-1192 from The Robert A. Welch Foundation and National Institutes of Health Grant HL 30050 (to B.S.S.M.) and National Institutes of Health Grants HL 50656 and HL 44603 (to S.S.G.). L.J.R. is the recipient of a Parker B. Francis Fellowship in Pulmonary Research.

1. Bredt, D. S. & Snyder, S. H. (1990) *Proc. Natl. Acad. Sci. USA* **87**, 682–685.
2. Bredt, D. S., Hwang, P. M., Glatt, C. E., Lowenstein, C., Reed, R. R. & Snyder, S. H. (1991) *Nature (London)* **351**, 714–718.
3. Lamas, S., Marsden, P. A., Li, G. K., Tempst, P. & Michel, T. (1992) *Proc. Natl. Acad. Sci. USA* **89**, 6348–6352.
4. Sessa, W. C., Harrison, J. K., Barber, C. M., Zeng, D., Durieux, M. E., D'Angelo, D. D., Lynch, K. R. & Peach, M. J. (1992) *J. Biol. Chem.* **267**, 15274–15276.
5. Xie, Q. W., Cho, H. J., Calayacay, J., Mumford, R. A., Swiderek, K. M., Lee, T. D., Ding, A., Troso, T. & Nathan, C. (1992) *Science* **256**, 225–228.
6. Lowenstein, C. J., Glatt, C. S., Bredt, D. S. & Snyder, S. H. (1992) *Proc. Natl. Acad. Sci. USA* **89**, 6711–6715.
7. Masters, B. S. S. (1994) *Annu. Rev. Nutr.* **14**, 131–145.
8. Bredt, D. S. & Snyder, S. H. (1994) *Annu. Rev. Biochem.* **63**, 175–195.
9. Dinerman, J. L., Lowenstein, C. J. & Snyder, S. H. (1993) *Circ. Res.* **73**, 217–222.
10. Schmidt, H. H. H. W., Pollock, J. S., Nakane, M., Gorsky, L. D., Förstermann, U. & Murad, F. (1991) *Proc. Natl. Acad. Sci. USA* **88**, 365–369.
11. Hevel, J. M., White, K. A. & Marletta, M. A. (1991) *J. Biol. Chem.* **266**, 22789–22791.
12. Stuehr, D. J., Cho, H. J., Kwon, N. S., Weise, M. F. & Nathan, C. (1991) *Proc. Natl. Acad. Sci. USA* **88**, 7773–7777.
13. Pollock, J. S., Förstermann, U., Mitchell, J. A., Warner, T. D., Schmidt, H. H. H. W., Nakane, M. & Murad, F. (1991) *Proc. Natl. Acad. Sci. USA* **88**, 10480–10484.
14. Förstermann, U., Pollock, J. S., Schmidt, H. H. H. W., Heller, M. & Murad, F. (1991) *Proc. Natl. Acad. Sci. USA* **88**, 1788–1792.
15. Cho, H. J., Xie, Q. W., Calaycay, J., Mumford, R. A., Swiderek, K. M., Lee, T. D. & Nathan, C. (1992) *J. Exp. Med.* **176**, 599–604.
16. Mayer, B., John, M., Heinzel, B., Werner, E. R., Wachter, H., Schultz, G. & Böhme, E. (1991) *FEBS Lett.* **288**, 187–191.
17. White, K. A. & Marletta, M. A. (1992) *Biochemistry* **31**, 6627–6631.
18. Stuehr, D. J. & Ikeda-Saito, M. (1992) *J. Biol. Chem.* **267**, 20547–20550.
19. McMillan, K., Bredt, D. S., Hirsch, D. J., Snyder, S. H., Clark, J. E. & Masters, B. S. S. (1992) *Proc. Natl. Acad. Sci. USA* **89**, 11141–11145.
20. Klatt, P., Schmidt, K. & Mayer, B. (1992) *Biochem. J.* **288**, 15–17.
21. Narhi, L. O. & Fulco, A. J. (1986) *J. Biol. Chem.* **261**, 7160–7169.
22. Charles, I. G., Chubb, A., Gill, R., Clare, J., Lowe, P. N., Holmes, L. S., Page, M., Keeling, J. G., Moncada, S. & Riveros-Moreno, V. (1993) *Biochem. Biophys. Res. Commun.* **196**, 1481–1489.
23. Richards, M. K. & Marletta, M. A. (1994) *Biochemistry* **33**, 14723–14732.
24. Barnes, H. J., Arlotto, M. P. & Waterman, M. R. (1991) *Proc. Natl. Acad. Sci. USA* **88**, 5597–5601.
25. Nishimoto, M., Clark, J. E. & Masters, B. S. S. (1993) *Biochemistry* **32**, 8863–8870.
26. Wynn, R. M., Davie, J. R., Zhi, W., Cox, R. P. & Chuang, D. T. (1994) *Biochemistry* **33**, 8962–8968.
27. Goloubinoff, P., Gatenby, A. A. & Lorimer, G. H. (1989) *Nature (London)* **337**, 44–47.
28. Gegner, J. A. & Dahlquist, F. W. (1991) *Proc. Natl. Acad. Sci. USA* **88**, 750–754.
29. Faeder, E. J. & Siegel, L. M. (1973) *Anal. Biochem.* **53**, 332–336.
30. McMillan, K. & Masters, B. S. S. (1993) *Biochemistry* **32**, 9875–9880.
31. McMillan, K. & Masters, B. S. S. (1995) *Biochemistry* **34**, 3686–3693.
32. Kelm, M. & Schrader, J. (1990) *Circ. Res.* **66**, 1561–1575.
33. Sheta, E. A., McMillan, K. & Masters, B. S. S. (1994) *J. Biol. Chem.* **269**, 15147–15153.
34. Gross, S. S. & Levi, R. (1992) *J. Biol. Chem.* **267**, 25722–25729.
35. Fukushima, T. & Nixon, J. C. (1980) *Anal. Biochem.* **102**, 176–188.
36. Rieske, J. S. (1967) *Methods Enzymol.* **10**, 488–493.
37. Wolff, D. J., Datto, G. A., Samatovicz, R. A. & Tempsick, R. A. (1993) *J. Biol. Chem.* **268**, 9425–9429.
38. Fisher, C. W., Shet, M. S., Caudle, D. L., Martin-Wixtrom, C. A. & Estabrook, R. W. (1992) *Proc. Natl. Acad. Sci. USA* **89**, 10817–10821.
39. Shet, M. S., Fisher, C. W., Arlotto, M. P., Shackleton, C. H. L., Holmans, P. L., Martin-Wixtrom, C. A., Saeki, Y. & Estabrook, R. W. (1994) *Arch. Biochem. Biophys.* **311**, 402–417.
40. Martin, J., Langer, T., Boteva, R., Schramel, A., Horwich, A. L. & Hartl, F. U. (1991) *Nature (London)* **352**, 36–42.
41. Klatt, P., Schmidt, K., Brunner, F. & Mayer, B. (1994) *J. Biol. Chem.* **269**, 1674–1680.

The material on this page was copied from the collection of the National Library of Medicine by a third party and may be protected by U.S. Copyright law.

EXHIBIT C

Proc. Natl. Acad. Sci. USA
Vol. 95, pp. 5795–5800, May 1998
Neurobiology

Amyloid β-peptide stimulates nitric oxide production in astrocytes through an NFκB-dependent mechanism

KEITH T. AKAMA†, CHRIS ALBANESE‡, RICHARD G. PESTELL‡, AND LINDA J. VAN ELDIK†§¶

†Department of Cell and Molecular Biology and §Northwestern Drug Discovery Program, Northwestern University Medical School, Chicago, IL 60611-3008; and ‡Department of Medicine and Developmental and Molecular Biology, Albert Einstein College of Medicine, Bronx, NY 10461

Communicated by Laslo Lorand, Northwestern University Medical School, Chicago, IL, February 26, 1998 (received for review December 29, 1997)

ABSTRACT **The major pathological features of Alzheimer's disease (AD) include amyloid plaques composed primarily of the β-amyloid (Aβ) peptide, degenerating neurons and neurofibrillary tangles, and the presence of numerous activated astrocytes and microglia. Although extensive genetic data implicate Aβ in the neurodegenerative cascade of AD, the molecular mechanisms underlying its effects on neurons and glia and the relationship between glial activation and neuronal death are not well defined. Aβ has been shown to induce glial activation, and a growing body of evidence suggests that activated glia contribute to neurotoxicity through generation of inflammatory cytokines and neurotoxic free radicals, such as nitric oxide (NO), potent sources of oxidative stress known to occur in AD. It is therefore crucial to identify specific Aβ-induced molecular pathways mediating these responses in activated glia. We report that Aβ stimulates the activation of the transcription factor NFκB in rat astrocytes, that NFκB activation occurs selectively from p65 transactivation domain 2, and that Aβ-induced NO synthase expression and NO production occur through an NFκB-dependent mechanism. This demonstration of how Aβ couples an intracellular signal transduction pathway involving NFκB to a potentially neurotoxic response provides a key mechanistic link between Aβ and the generation of oxidative damage. Our results also suggest possible molecular targets upon which to focus future drug discovery efforts for AD.**

Alzheimer's disease (AD) is a neurodegenerative disorder resulting in progressive neuronal death and memory loss. Neuropathologically, the disease is characterized by neurofibrillary tangles and neuritic plaques composed of aggregates of β-amyloid (Aβ) protein, a 40–43 amino acid proteolytic fragment derived from the amyloid precursor protein. The importance of Aβ in AD has been shown by means of several transgenic animal studies. The overexpression of mutant amyloid precursor protein results in neuritic plaque formation and synapse loss (1) and correlative memory deficits, as well as behavioral and pathological abnormalities similar to those found in AD (2).

Neuritic plaques in AD are densely surrounded by reactive astrocytes (3, 4). These reactive astrocytes participate in the inflammatory response observed in AD by their production of proinflammatory cytokines such as interleukin 1β (5), and by their expression of inducible nitric oxide synthase (iNOS) (6, 7). iNOS generates nitric oxide (NO) and NO-derived reactive nitrogen species such as peroxynitrite. One possible pathology of AD therefore can be viewed as the accumulation of such free radicals during inflammation resulting in lipid peroxidation, tyrosine nitrosylation, DNA oxidative damage, and ultimately neuronal destruction within the brain (8–11). Understanding the expression of iNOS in the AD brain is therefore critical. NOS immunoreactivity has been observed near Aβ neuritic plaques (7), and iNOS expression can be stimulated in cultured astrocytes or microglia by Aβ (6, 12–15). This Aβ stimulation of iNOS can result in the production of excessive amounts of diffusible NO, which when converted to peroxynitrite, becomes a powerfully detrimental oxidant with direct cytopathological consequences (16).

Relatively little is known about the molecular mechanisms governing Aβ stimulation of astrocyte iNOS activity. One candidate pathway involves the transcription factor NFκB (17). NFκB is a heterodimeric transcription factor composed of subunits from the Rel family of proteins. It is located in the cytoplasm as an inactive complex when associated with its inhibitor IκB, which masks the NFκB nuclear localization signal. Upon stimulation by cytokines or cellular stress, NFκB can be rapidly activated by the phosphorylation of IκB at serine residues, which direct IκB for proteosome-mediated degradation (18). The activated NFκB heterodimer is then free to translocate into the nucleus and bind to specific 10-bp response elements of target genes, typically found in inflammation-responsive genes. The iNOS promoter contains at least one NFκB response element (19), and activated NFκB is an important transcription factor in iNOS gene expression in response to cytokines or cellular stress (20). Recently, NFκB was observed immunohistochemically in postmortem AD brain (21).

We report here that Aβ activates NFκB in cultured rat astrocytes and demonstrate that Aβ stimulation of iNOS expression and NO production occurs through an NFκB-dependent mechanism. These data define a specific molecular pathway that links Aβ activation of glia to a potentially neurotoxic oxidative stress response, and support the concept that Aβ-induced oxidative damage is neuropathogenic in AD.

MATERIALS AND METHODS

Cell Culture and Amyloid β 1–42 Peptide (Aβ42) Preparation. Cultured rat cortical astrocytes were prepared and tertiary cultures made as described (22). Cells were maintained in αMEM supplemented with 10% fetal bovine serum (FBS) (HyClone) and antibiotics [100 units/ml penicillin/100 μg/ml streptomycin (GIBCO/BRL)]. Twenty-four hours before stimulation, astrocyte medium was removed, cells were washed once with prewarmed PBS, and then serum-free αMEM containing N2 media supplement (GIBCO/BRL) was added to the cultures. Aβ peptides [Aβ 1–42 or scrambled 1–42 sequence (Aβ42scr) KVKGLIDGAHIGDLVYEFMD-SNSAIFREGVGAGHVHVAQVEF] were either purchased

The publication costs of this article were defrayed in part by page charge payment. This article must therefore be hereby marked "*advertisement*" in accordance with 18 U.S.C. §1734 solely to indicate this fact.

© 1998 by The National Academy of Sciences 0027-8424/98/955795-6$2.00/0
PNAS is available online at http://www.pnas.org.

Abbreviations: Aβ42, amyloid β 1–42 peptide; Aβ42scr, scrambled Aβ1–42 sequence; AD, Alzheimer's disease; EMSA, electrophoretic mobility-shift assay; iNOS, inducible nitric oxide synthase; TAD, transactivating domain; RLU, relative light unit.

¶To whom reprint requests should be addressed at: Northwestern University Medical School, W-129, 303 East Chicago Avenue, Chicago, IL 60611-3008. e-mail: vaneldik@nwu.edu.

The material on this page was copied from the collection of the National Library of Medicine by a third party and may be protected by U.S. Copyright law.

(Bachem) or prepared as described previously (6). Aβ peptides were aggregated as described previously (6). Briefly, a 20× Aβ peptide stock was subjected to 2-day acidic aging conditions (200 μM Aβ in 1 mM HCl) at room temperature, or a 10× Aβ stock was subjected to 1-day neutral aging conditions (100 μM Aβ in αMEM/0.2% dimethyl sulfoxide) at 4°C. The aggregated Aβ stocks contained both fibrillar species and globular oligomeric aggregates by atomic force microscopy. The Aβ stocks were then added to the cultures at the appropriate stimulus concentration.

Electrophoretic Mobility-Shift Assays (EMSA). Nuclear extracts from treated astrocytes were prepared by a modified Dignam method (23). Briefly, treated cells (10^6 cells per 60-mm dish) were scraped into ice-cold PBS supplemented with 1 mM phenylmethylsulfonyl fluoride (PMSF). Cells were pelleted in microfuge tubes and resuspended in 400 μl of ice-cold low-salt buffer A (10 mM Hepes, pH 7.9/1.5 mM $MgCl_2$/10 mM KCl). After 10 min on ice, 25 μl of 10% Nonidet P-40 was added and the samples were vortexed vigorously for 10 sec. Samples were centrifuged (13,000 × *g*) for 30 sec at 4°C, and the pellet was resuspended in 30 μl of ice-cold high-salt buffer C (20 mM Hepes, pH 7.9)/25% glycerol/420 mM NaCl/1.5 mM $MgCl_2$/0.2 mM EDTA). Resuspended pellets were allowed to rock gently at 4°C for 30 min and then centrifuged at 4°C for 15 min. The supernatant (nuclear extract) was saved and protein concentration was determined by Bradford assay. Before using both buffer A and buffer C, a fresh mixture of inhibitors was added to each at a final concentration of 1 mM PMSF, 1 μg/ml leupeptin A, 1 mM DTT, and 1 mM sodium orthovanadate. Binding reactions were assayed in 20 μl volumes by incubating 3 μg of nuclear extract with reaction buffer [50 mM Tris·HCl, pH 7.5/5 mM EDTA/2.5 mM DTT/250 mM NaCl/0.25 mg/ml poly(dI·dC)·poly(dI·dC) (Pharmacia)]. For competition, unlabeled specific (identical NFκB oligonucleotide shift probe) or nonspecific (AP2 oligonucleotide shift probe) (Promega) probes were allowed to incubate with appropriate samples in 50-fold molar excess for 10–15 min before incubating all samples with ^{32}P-labeled oligonucleotide shift probes (approximately 50,000–200,000 cpm) at room temperature for 20 min. "Super-shifting" was conducted by then incubating the appropriate samples with Rel family antibodies (6 μg per sample) for 45 min at room temperature. Supershift polyclonal antibodies against synthetic peptides from the NFκB/Rel family of proteins p65(RelA), p50, p52, c-Rel(p75), and RelB(p68) were purchased from Santa Cruz Biotechnology. Products were subjected to electrophoresis at 200 V in a 4°C room for approximately 90 min on 5.5% nondenaturing polyacrylamide gels in high ionic strength TGE buffer (50 mM Tris·HCl/380 mM glycine/2 mM EDTA, pH ≈8.5). Lanes with samples were devoid of any loading dyes, which interfere with the binding reactions. Dried gels were exposed to Storm Phosphor Imaging plates (Molecular Dynamics) and viewed by IMAGEQUANT software (Molecular Dynamics). To size EMSA figures to page, the vertical aspect ratio of each picture was reduced by approximately 50%. Oligonucleotides representing the NFκB response element (consensus sequence, 5′-AGT TGA GGG GAC TTT CCC AGG C-3′) were purchased from Promega. Mutant NFκB (NFκBmut) response element oligonucleotides (5′-AGT TGA GGC* GAC TTT CCC AGG C-3′, where * denotes mutated base) were purchased from Santa Cruz Biotechnology. To prepare gel shift probes, oligonucleotides were labeled with [γ-^{32}P]ATP (Amersham) by using T4 polynucleotide kinase by the protocol provided (gel shift assay system, Promega). Unincorporated nucleotides were removed by Centri-Sep spin columns (Princeton Separations).

Plasmids. 3xRel-LUC was a gift from M. L. Scott and D. Baltimore (Massachusetts Institute of Technology) and contains three tandem Ig κB repeats from the construct −55 to +19 hIFNβ-CAT (24), which were cloned into the *Not*I–*Hin*dIII site of pBL, and thereby linked to the luciferase reporter gene. CMV-IκB(Super-repressor) [CMV-IκB(Sr)] was generously provided by Dean Ballard (Howard Hughes Medical Institute, Vanderbilt University Medical Center). IκB was cloned into the expression vector pCMV-4, and serine residues 32 and 36 (sites of phosphorylation that precede IκB degradation) have been mutated to alanines (25). pXP2 backbone vector and 7kb(wt) iNOS-LUC were kindly provided by David Geller (University of Pittsburgh) and have been described (26). PCR site-directed mutagenesis (QuikChange, Stratagene) was used to mutate the NFκB response element immediately upstream of the TATAA box of the 7kb(wt) iNOS-LUC promoter construct (GGG to CTC) to generate the 7kb(NFκB$^-$) iNOS-LUC promoter construct. DNA sequence analysis confirmed the mutation in the response element and verified the absence of any additional mutations. UAS(5x)-E1B-TATA-LUC (UAS-LUC) contains five tandem repeats of the Gal4 upstream activating sequence cloned pA3-LUC and has been described (27).

Transient Transfections. Astrocytes were transfected by using the synthetic cationic lipid Tfx-50 (Promega) or by SuperFect transfection reagent (Qiagen, Chatsworth, CA).

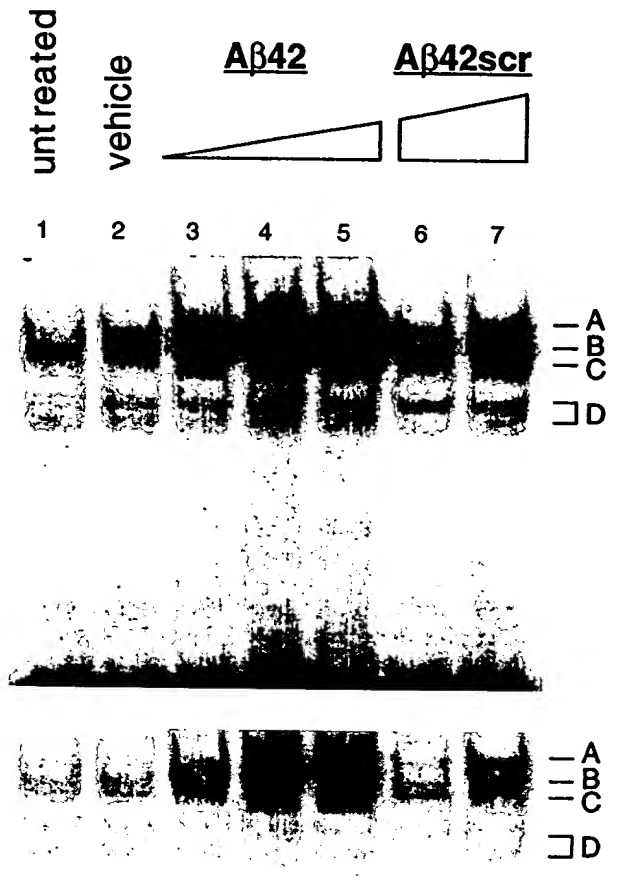

FIG. 1. Aβ42 activates NFκB in a dose-dependent manner. Nuclear extracts from astrocytes stimulated by increasing doses of Aβ42 were incubated with ^{32}P-labeled NFκB oligonucleotide probe for gel mobility-shift assay. Lanes: 1, untreated astrocyte nuclear extract; 2, vehicle-treated nuclear extract (0 μM Aβ42); 3–5, 1 μM, 5 μM, and 10 μM Aβ42, respectively. As a peptide control, nuclear extracts from astrocytes stimulated by a scrambled Aβ42 peptide [10 μM Aβ42scr (lane 6) and 20 μM Aβ42scr (lane 7)] were run to demonstrate the activation specificity of Aβ42. Cells were treated for 12 hr, a time-point where maximal NFκB activation could be detected by EMSA (data not shown). NFκB activation complexes are indicated by A–D. (*Lower*) A shorter exposure of the autoradiogram to allow better visualization of the individual complexes in lanes 4 and 5.

The material on this page was copied from the collection of the National Library of Medicine by a third party and may be protected by U.S. Copyright law.

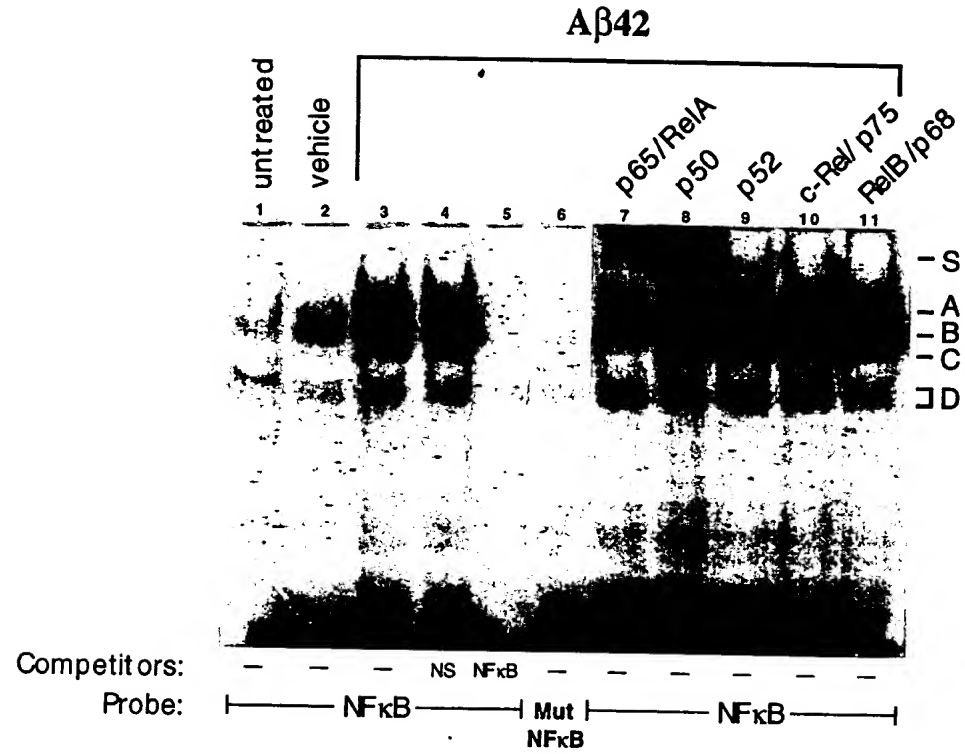

FIG. 2. Specificity of Aβ42-activated NFκB. Gel mobility-shift assay with nuclear extracts prepared from untreated astrocytes (lane 1), vehicle-control-treated astrocytes (lane 2), and 10 μM Aβ42-treated astrocytes (lanes 3–11). Cells were incubated for 12 hr. ^{32}P-labeled oligonucleotide shift probes used contained consensus NFκB response element (lanes 1–3 and 7–11), 50-fold molar excess of unlabeled AP2 (nonspecific competitor, NS) shift probe before ^{32}P-labeled NFκB shift probe (lane 4), approximately 50-fold molar excess of unlabeled NFκB (specific competitor, NFκB) shift probe before ^{32}P-labeled NFκB shift probe (lane 5), or ^{32}P-labeled mutant NFκB carrying a 1-bp substitution within the NFκB response element (lane 6). Polyclonal antibodies used to detect the indicated Rel family subunits are as indicated (lanes 7–11). NFκB activation complexes are indicated by A–D. Supershifted complexes are indicated by S and were detected only in samples incubated with either p65/RelA or p50 antibody.

Optimized DNA/reagent ratios were determined to be 1:1 (micrograms DNA/lipid charge) for Tfx-50, and 1:1 (micrograms DNA/microliters reagent) for SuperFect. All DNA used in transfections were prepared by the endotoxin-free plasmid prep (Endo-Free Maxi-prep kits, Qiagen). For transfections, secondary astrocytes were trypsinized and replated into 12-well or 48-well tissue culture plates (1.5×10^5 cells per well for 12-well plates, 1×10^4 cells per well for 48-well plates). Cells were immediately exposed to DNA transfecting complexes for 1–2 hr at 37°C. Transfecting complexes were then removed, cells washed once with warm PBS, and incubated for 4–6 hr in αMEM (with 20% FBS). This medium was then replaced with αMEM containing 10% FBS, and cells were incubated overnight before changing the medium to serum-free N2-supplemented αMEM for 24 hr before stimulation. For luciferase assays after the appropriate stimulus, cells were rinsed once with ice-cold PBS and immediately lysed for 5 min at 4°C in lysis buffer (0.5 M Hepes, pH 7.4/5% Triton N-101/1 mM $CaCl_2$/1 mM $MgCl_2$). Lysates were transferred to 96-well black-walled plates (Corning Costar), and an equal volume of reconstituted LucLite luciferase substrate (Packard) was added to each sample. Luciferase reactions were allowed to proceed for approximately 5 min at room temperature before quantitating relative light unit (RLU) output on a LumiCount (Packard) high-throughput luminometer (20-sec reads per sample well). Blank transfections (unstimulated astrocytes transfected with the appropriate backbone vector) were included for each experiment to determine machine noise background, which was then subtracted before data analysis. Each set of data represents results from 6–11 experiments.

Nitrite Assays. Nitrite production by astrocytes was measured by Griess assay as a read-out for iNOS activity as described previously (22). Astrocytes were treated with various stimuli in a total volume of 100 μl per well in a 48-well plate, and 80 μl of conditioned medium was collected after 48 hr of stimulus. To measure total nitrite produced in a 48-hr period, any nitrate in the conditioned medium was first reduced back to nitrite with nitrate reductase and NAPDH (Sigma) at 37°C for 1 hr. An equal volume of Griess reagent [0.5% sulfanilamide and 0.05% *N*-(1-naphthyl) ethylenediamine] was then added to the conditioned medium and the reaction was allowed to proceed for 5 min at room temperature before the absorbance at 540 nm was measured. A sodium nitrite linear range standard curve from 0 to 75 μM nitrite was used to determine the concentration of nitrite in the astrocyte conditioned medium.

RESULTS

To characterize the activation state of NFκB in astrocytes stimulated by Aβ42, we performed EMSA assays on isolated nuclear extracts incubated with ^{32}P-labeled oligonucleotide probes containing the 10-bp consensus sequence of the NFκB response element.

Four mobility-shifted complexes were observed using nuclear extracts from astrocytes treated with Aβ42 (Fig. 1, lanes 3, 4, and 5, bands A–D). Bands A, B, and C exhibited a dose-dependent increase in binding, beginning with nuclear extracts from cells treated with 1 μM Aβ42 (Fig. 1, lane 3). In contrast, nuclear extracts from cells treated with a scrambled Aβ42 peptide sequence (Aβ42scr) exhibited only a modest gel shift at double the maximum concentration of Aβ42 (Fig. 1, lane 7).

The material on this page was copied from the collection of the National Library of Medicine by a third party and may be protected by U.S. Copyright law.

The specificity of the NFκB response was characterized further by EMSA. Compared with controls (Fig. 2, lanes 1 and 2), NFκB was strongly activated in astrocytes stimulated by Aβ42 (Fig. 2, lane 3). Maximal enhancement of binding was observed by 12 hr after Aβ activation (data not shown). All four bands could be competed away by specific competitor probe (50-fold molar excess of cold cognate competitor; Fig. 2, lane 5) but not by nonspecific probe (50-fold molar excess of unlabeled oligo shift probe containing the AP2 binding site; Fig. 2, lane 4). In addition, a mutant oligonucleotide probe that included a 1-bp substitution in the NFκB response element sequence exhibited little if any gel shift activity (Fig. 2, lane 6). Lysates from Aβ-activated astrocytes assayed by Western immunoblotting revealed the presence of all five protein members of the Rel family (data not shown). "Super-shifts," conducted with a panel of antibodies specific for each Rel family member, identified p65/RelA and p50 within the complex (Fig. 2, lanes 7–11). Bands A, B, and C were shifted by the antibodies to p65/RelA and p50, but not by the antibodies to p52, c-Rel/p75, or RelB/p68. Band D was unaffected by any of these Rel family antibodies.

The activation of NFκB was also determined by using the luciferase NFκB reporter construct 3xRel-LUC. This reporter construct has three tandem NFκB response element repeats upstream of a minimal promoter driving the luciferase gene.

Aβ42 treatment induced 3xRel-LUC approximately 4.5-fold over the levels in untreated or vehicle-treated cells (Fig. 3*A*). Aβ42scr did not stimulate 3xRel-LUC reporter expression levels above untreated or vehicle-treated cells (Fig. 3*A*). 3xRel-LUC reporter specificity for NFκB was verified by cotransfection with CMV-IκB(Sr), an IκB "super-repressor" expression construct. In this construct, IκB serines 32 and 36 have been mutated to alanines, preventing the protein from being phosphorylated, thereby blocking its degradation and thus strongly maintaining inhibition of NFκB activity. Overexpression of IκB(Sr) blocked Aβ42-dependent 3xRel-LUC activity to levels equivalent to unstimulated cells (Fig. 3*B*).

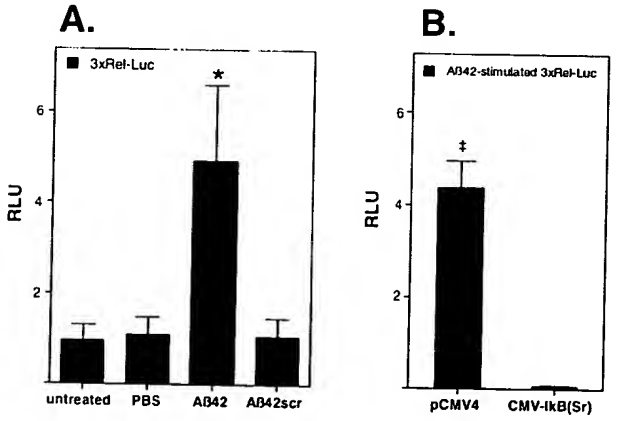

FIG. 3. Aβ42-specific stimulation of NFκB reporter gene activation. (*A*) The 3xRel-LUC plasmid (three tandem NFκB response element repeats with a minimal promoter cloned upstream of the luciferase gene) was transfected into astrocytes, which were then left untreated or stimulated for 12 hr by either PBS, 10 μM Aβ42, or 10 μM Aβ42scr. Luciferase expression in Aβ42-stimulated cells was significantly increased above that in untreated, PBS-treated, or Aβ42scr-treated cells. Data shown (mean ± SEM) represent $n = 8$ transfections and are RLUs. (*B*) Cotransfecting the 3xRel-LUC construct with the IκB (Super-repressor, Sr) expression construct [CMV-IκB(Sr)] reduced Aβ-stimulated 3xRel-LUC luciferase activity to near background levels compared with cotransfection of 3xRel-LUC with the backbone vector pCMV4. *, Significantly different from PBS control ($P < 0.05$); ‡, significantly different from control vector ($P < 0.005$). Statistics here and results throughout have been calculated by Student's *t* test. Significance is determined if $P < 0.05$.

Because p65/RelA was a participating subunit of NFκB, a subunit known to have at least two different transactivating domains (TADs) (28), we used two p65 TADs in yeast Gal4-dependent reporter constructs to determine which domain(s) specifically participated in Aβ42-stimulated NFκB activation. NFκB(1)-Gal4 included TAD1 of p65, which contains amino acid residues 520–590, and NFκB(2)-Gal4 included TAD2 of p65, which contains amino acid residues 286–518 (29). Either construct was cotransfected with a luciferase reporter construct containing five tandem repeats of the yeast Gal4-UAS binding site. As shown in Fig. 4, Aβ42 stimulated NFκB(2)-Gal4 2- to 3-fold, whereas cells transfected with NFkB(1)-Gal4 showed no induction. In addition, transfected cells treated with Aβ42scr showed no significant activity from either TAD1 or TAD2 of p65. Therefore, NFκB activation by Aβ42 is selectively regulated at the amino acid region of p65/RelA TAD 2.

We have previously shown that Aβ42 can enhance iNOS mRNA expression and nitrite production in cultured astrocytes (6). To characterize the potential importance of Aβ-activated NFκB for iNOS activity, we used several approaches. Astrocytes transfected with a human 7-kb iNOS promoter-luciferase construct [7kb(wt) iNOS-LUC] exhibited an approximate 7- to 10-fold increase in luciferase activity in Aβ42-activated astrocytes compared with vehicle-treated or untreated astrocytes (Fig. 5*A Left*). This Aβ-induced increase in iNOS promoter activity was almost completely abolished upon mutation of the proximal NFkB response element (5′-GGGACACTCC-3′ to 5′-CTCACACTCC 3′) (Fig. 5*A Right*). However, despite a reduction in basal level activity, the 7kb(NFκB⁻) iNOS-LUC promoter construct responds to stimulation by 1 mM dibutyryl cAMP in a fashion indistinguishable to that of the 7kb(wt) iNOS-LUC construct (data not shown), demonstrating that NFκB-independent signaling pathways were unaffected by mutation of the NFκB binding site. Furthermore, cotransfection with CMV-IκB(Sr) abrogated Aβ-stimulated luciferase activity of the 7-kb iNOS-LUC promoter construct (Fig. 5*B*)

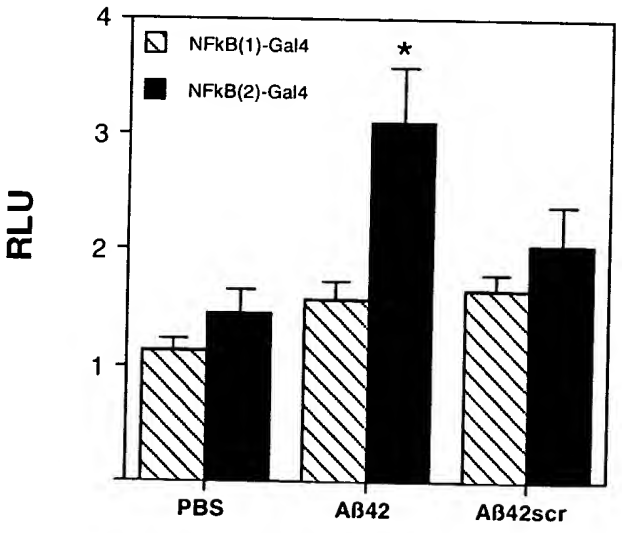

FIG. 4. Aβ42 activates NFκB at p65/RelA TAD 2. NFκB(1)-Gal4 and NFκB(2)-Gal4 expression constructs containing the first and second TADs of p65/RelA, respectively, were individually cotransfected with the yeast Gal4-UAS luciferase reporter plasmid to determine from which domain NFκB activation by Aβ42 occurred. Ten micromolar Aβ42-stimulated astrocytes showed approximately 2- to 3-fold more NFκB(2)-Gal4 luciferase activity compared with PBS-treated or 10 μM Aβ42scr-treated cells. There was no significant stimulation of NFκB(1)-Gal4 in Aβ42-treated cells compared with PBS-treated or 10 μM Aβ42scr-treated cells. *, Significantly different from PBS control ($P < 0.005$).

The material on this page was copied from the collection of the National Library of Medicine by a third party and may be protected by U.S. Copyright law.

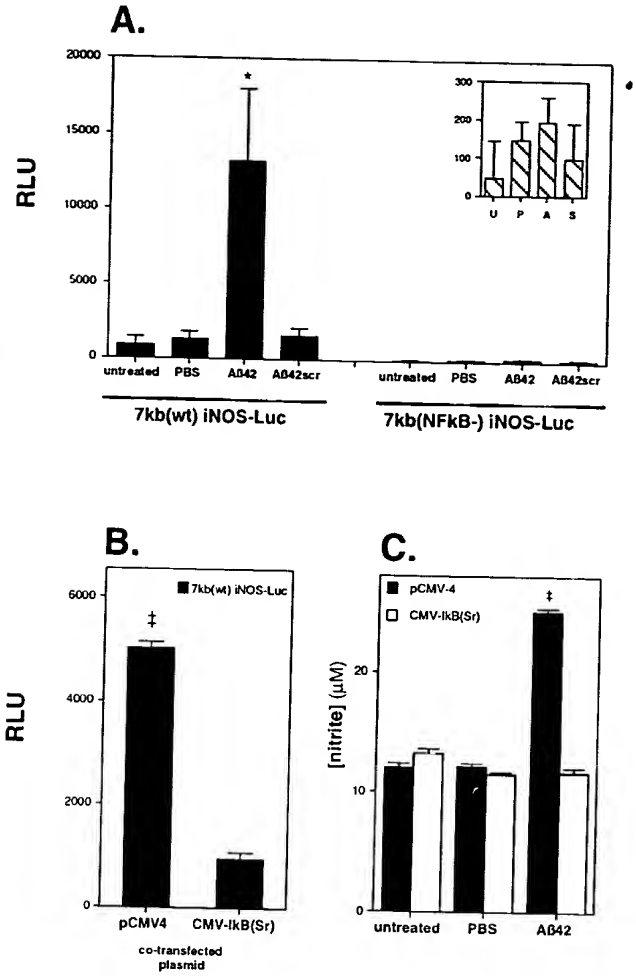

FIG. 5. Aβ42 stimulates iNOS in astrocytes in an NFκB-dependent manner. (*A*) Aβ42-stimulated iNOS promoter activity as determined by luciferase activity. Astrocytes were transfected with the 7-kb iNOS promoter luciferase reporter construct [7kb(wt) iNOS-LUC] and then either left untreated or stimulated by PBS, 10 μM Aβ42, or 10 μM Aβ42scr for 12 hr. Only Aβ42 significantly stimulated iNOS promoter activity. Inactivation of the TATAA-box proximal NFκB response element in the 7-kb iNOS promoter by site-directed mutagenesis [7kb(NFκB$^-$) iNOS-LUC] results in no significant promoter activity by Aβ42. (*Inset*) The same 7kb(NFκB$^-$) iNOS-LUC RLU data with a more focused ordinate range. U, P, A, and S are untreated, PBS-, Aβ42-, and Aβ42scr-treated cells, respectively. Data (mean RLU ± SEM) represent n = 8 transfections. (*B*) Cotransfecting the 7-kb iNOS-LUC construct with CMV-IκB(Sr) reduced Aβ-stimulated iNOS promoter activity to near background levels compared with cotransfection of 7kb(wt) iNOS-LUC with the backbone vector pCMV4. Data (mean RLU ± SEM) represent n = 6 transfections. (*C*) iNOS activity was determined by measuring the production of nitrite by a modified Griess assay as described. Aβ42-stimulated nitrite production was reduced to background control levels in astrocytes transfected with CMV-IκB(Sr), but not in Aβ42-stimulated astrocytes transfected with backbone vector pCMV4 alone. (Each transfection well received a total of 750 ng of plasmid DNA. Control backbone vector transfection wells received 750 ng of pCMV4 and CMV-IκB(Sr) transfection wells received 0.75 ng of CMV-IκB(Sr) plus 749.25 ng of pCMV4.) Data (mean ± SEM) represent n = 11 transfections. *, Significantly different from PBS control ($P < 0.05$); ‡, significantly different from CMV-IκB(Sr) ($P < 0.005$).

and NO production, as measured by the stable metabolites nitrite and nitrate (Fig. 5*C*). These three approaches demonstrate that Aβ42 stimulation of iNOS expression and NO production is NFκB-dependent.

DISCUSSION

We report here that the neurotoxic 42-aa Aβ peptide stimulates the activation of the transcription factor NFκB in cultured rat astrocytes in a dose-dependent manner, whereas a scrambled-sequence Aβ42 peptide at an equal concentration does not. Although expression of all five NFκB/Rel proteins can be detected in astrocytes, only specific Rel family members (p50 and p65/RelA) participate in Aβ activation. Moreover, Aβ42 stimulation of NFκB occurs selectively from TAD 2 of p65/RelA and not from TAD 1. Last, Aβ42 stimulation of iNOS gene expression and NO production is almost completely NFκB dependent.

Nitrogen species such as NO and NO-derived peroxynitrite are strong inducers of oxidative stress. It is therefore important to understand the molecular mechanisms underlying NO activation in an attempt to slow or prevent oxidative injury to the brain. This is emphasized by initial studies on dementia onset and the use of anti-inflammatory drugs and antioxidants (30–32). Chronic antioxidant usage, which may curb oxidative damage to cells, appears to result in a delay of dementia in AD patients. A prominent source of the oxidative damage seen in AD is peroxynitrite (16). Our results are consistent with previous studies that have shown that iNOS expression and peroxynitrite damage occur throughout the AD brain (8), and that NFκB activation can be observed in AD brain sections (21). However, our data couple Aβ42-stimulated NFκB activation in AD to the production of iNOS and NO. These studies provide direct support for the postulation (33) of a neurotoxic role for NFκB in AD in the context of glia and suggest that in AD, NFκB is not "protective" in glia as it can be in neurons (34). These studies also provide a model for how glia participate in the oxidative damage widely seen in AD and allow a focus on specific signaling pathways involving p65/RelA. Aβ42 exposure likely influences multiple signal transduction pathways, some of which ultimately can lead to enhanced NO production and subsequent oxidative damage. It should also be noted that other Aβ42-stimulated signal transduction pathways not involving NFκB or NO may lead to oxidative injury. Nevertheless, our data, which strongly implicate TAD 2 of NFκB p65/RelA in the induction of NO production by Aβ42 and therefore potential oxidative injury to the brain, may provide new therapeutic approaches to AD.

We thank the laboratory of Dr. D. Martin Watterson for assistance with peptide production and characterization. These studies were supported in part by National Institutes of Health Grants AG13939 and GM30861.

1. Masliah, E., Sisk, A., Mallory, M., Mucke, L., Schenk, D. & Games, D. (1996) *J. Neurosci.* **16**, 5796–5811.
2. Hsiao, K., Chapman, P., Nilsen, S., Eckman, C., Harigaya, Y., Younkin, S., Yang, F. & Cole, G. (1996) *Science* **274**, 99–102.
3. Selkoe, D. J. (1991) *Neuron* **6**, 487–498.
4. Griffin, W. S. T. & Stanley, L. C. (1993) in *Biology and Pathology of Astrocyte-Neuron Interactions*, ed. Federoff, S. (Plenum, New York), pp. 359–381.
5. Mrak, R. E., Sheng, J. G. & Griffin, W. S. T. (1995) *Human Pathol.* **26**, 816–823.
6. Hu, J., Akama, K. T., Krafft, G. A., Chromy, B. A. & Van Eldik, L. J. (1998) *Brain Res.* **785**, 195–206.
7. Wallace, M. N., Geddes, J. G., Farquhar, D. A. & Masson, M. R. (1997) *Exp. Neurol.* **144**, 266–272.
8. Smith, M. A., Richey-Harris, P. L., Sayre, L. M., Beckman, J. S. & Perry, G. (1997) *J. Neurosci.* **17**, 2653–2657.
9. Mattson, M. P. (1997) *Alzheimer's Disease Rev.* **2**, 1–14.
10. Hensley, K., Butterfield, D. A., Hall, N., Cole, P., Subramaniam, R., Mark, R., Mattson, M. P., Markesbery, W. R., Harris, M. E., Aksenov, M., Aksenova, M., Wu, J. F. & Carney, J. M. (1996) *Ann. N.Y. Acad. Sci.* **34**, 120–134.
11. Van Dyke, K. (1997) *Med. Hypotheses* **48**, 375–380.
12. Rossi, F. & Bianchini, E. (1996) *Biochem. Biophys. Res. Commun.* **225**, 474–478.

The material on this page was copied from the collection of the National Library of Medicine by a third party and may be protected by U.S. Copyright law.

13. Meda, L., Cassatella, M. A., Szendrei, G. I., Otvos, L., Baron, P., Villalba, M., Ferrari, D. & Rossi, F. (1995) *Nature (London)* **374,** 647–650.
14. Goodwin, J. L., Uemura, E. & Cunnick, J. E. (1995) *Brain Res.* **692,** 207–214.
15. Ii, M., Sunamoto, M., Ohnishi, K. & Ichimori, Y. (1996) *Brain Res.* **720,** 93–100.
16. Beckman, J. S. & Koppenol, W. H. (1996) *Am. J. Physiol.* **271,** C1424–C1437.
17. Xie, Q., Kashiwabara, Y. & Nathan, C. (1994) *J. Biol. Chem.* **269,** 4705–4708.
18. Thanos, D. & Maniatis, T. (1995) *Cell* **80,** 529–532.
19. Nunokawa, Y., Ishida, N. & Tanaka, S. (1994) *Biochem. Biophys. Res. Commun.* **200,** 802–807.
20. O'Neill, L. A. J. & Kaltschmidt, C. (1997) *Trends Neurosci.* **20,** 252–258.
21. Terai, K., Matsuo, A., McGeer, E. G. & McGeer, P. L. (1996) *Brain Res.* **739,** 343–349.
22. Hu, J., Castets, F., Guevara, J. L. & Van Eldik, L. J. (1996) *J. Biol. Chem.* **271,** 2543–2547.
23. Andrews, N. C. & Faller, D. V. (1991) *Nucleic Acids Res.* **19,** 2499.
24. Fujita, T., Shibuya, H., Hotta, H., Yamanishi, K. & Taniguchi, T. (1987) *Cell* **49,** 357–367.
25. Brockman, J. A., Scherer, D. C., McKinsey, T. A., Hall, S. M., Qi, X., Lee, W. Y. & Ballard, D. W. (1995) *Mol. Cell. Biol.* **15,** 2809–2818.
26. deVera, M. E., Shapiro, R. A., Nussler, A. K., Mudgett, J. S., Simmons, R. L., Morris, S. M., Jr., Billar, T. R. & Geller, D. A. (1996) *Proc. Natl. Acad. Sci. USA* **93,** 1054–1059.
27. Watanabe, G., Howe, A., Lee, R. J., Albanese, C., Shu, I.-W., Karnezis, A. N., Zon, L., Kyriakis, J., Rundell, K. & Pestell, R. G. (1996) *Proc. Natl. Acad. Sci. USA* **93,** 12861–12866.
28. Schmitz, M. L., dos Santos Silva, M. A. & Baeuerle, P. A. (1995) *J. Biol. Chem.* **270,** 15576–15584.
29. Seipel, K., Georgiev, O. & Schaffner, W. (1992) *EMBO J.* **11,** 4961–4968.
30. Breitner, J. C. (1996) *Annu. Rev. Med.* **47,** 401–411.
31. Sano, M., Ernesto, C., Thomas, R. G., Klauber, M. R., Schafer, K., Grundman, M., Woodbury, P., Growdon, J., Cotman, C. W., Pheiffer, E., Schneider, L. S. & Thal, L. J. (1997) *N. Engl. J. Med.* **336,** 1216–1222.
32. Stewart, W. F., Kawas, C., Corrada, M. & Metter, E. J. (1997) *Neurology* **48,** 626–632.
33. Kaltschmidt, B., Uherek, M., Volk, B., Baeuerle, P. A. & Kaltschmidt, C. (1997) *Proc. Natl. Acad. Sci. USA* **94,** 2642–2647.
34. Barger, S. W., Horster, D., Furukawa, K., Goodman, Y., Krieglstein, J. & Mattson, M. P. (1995) *Proc. Natl. Acad. Sci. USA* **92,** 9328–9332.

The material on this page was copied from the collection of the National Library of Medicine by a third party and may be protected by U.S. Copyright law.

04/25/2002 11:04 30165F PAGE 05

EXHIBIT D

)LOGY INTERNATIONAL

Vol. 35, No. 6, May 1995 BIOCHEMISTRY *and* MOLECULAR BIOLOGY INTERNATIONAL
Pages 1339–1348

The material on this page was copied from the collection of the National Library of Medicine by a third party and may be protected by U.S. Copyright law.

em. 230, 707-
f. Biochem. 1,
rs. Acta 158,
irochem. 17,
Neurochem. 44,
rs. Acta 212,
J. (1951)
id Kodama H.
mmunol. Methods
-1224.
arese R. M.,
91) Eur. J.

ACTIVATION OF NEURONAL NITRIC OXIDE SYNTHASE BY FLAVIN ADENINE DINUCLEOTIDE

Akiko Hashida-Okumura, Katsuya Nagai, Nobuaki Okumura and Hachiro Nakagawa

Division of Protein Metabolism, Institute for Protein Research, Osaka University, 3-2, Yamada-Oka, Suita, Osaka 565, Japan

Received December 26, 1994

Summary. Bovine adrenals were found to contain a factor that activates neuronal nitric oxide synthase (NOS) and reduces the blood pressure when injected into the lateral cerebral ventricle (LCV). This factor showed chemical and functional characteristics similar to flavin adenine dinucleotide (FAD). Therefore, the effect of FAD on neuronal NOS activity was examined. FAD caused at least 2-fold stimulation of NOS partially purified from rat brain. This effect was not simply due to formation of the holoenzyme. Kinetic analyses showed that NOS exhibited negative cooperativity with *L*-arginine, its substrate, and FAD counteracted this effect. Furthermore, injection of FAD into the LCV reduced the blood pressure. These results suggest that FAD stimulates neuronal NOS by counteracting its negative cooperativity with *L*-arginine and also lowers the blood pressure by activating NOS.

INTRODUCTION

Nitric oxide (NO) is an inorganic free radical with many physiological and pathological functions such as in vasodilatation, neurotransmission and cytotoxicity (1-3). NO is synthesized by nitric oxide synthase (EC 1.14.13.39, NOS) , which is classified into at least three types. Neuronal NOS (4) and endothelial NOS (5) are constitutively expressed in neuronal tissues and vascular endothelial cells, respectively. On the other hand, inducible NOS is expressed in macrophages (6), hepatocytes (7), vascular smooth muscle cells (8) and other cells and is induced by cytokines. Neuronal NOS utilizes *L*-arginine as a substrate and requires NADPH, calcium, calmodulin, tetrahydrobiopterin, flavin mononucleotide (FMN) and flavin adenine dinucleotide (FAD) as cofactors. There are reports that neuronal NOS

1039-9712/95/061339-10$05.00/0
Copyright © 1995 by Academic Press Australia.
All rights of reproduction in any form reserved.

04/25/2002 11:04 3016567246 TOP SHELF INC PAGE 06

has a binding site for FAD (9) and that purified neuronal NOS contains tightly noncovalently bound FAD (10,11), which might play a role in the transfer of electrons.

We found a factor in rat urine and bovine adrenals that activated neuronal NOS (12). Its injection into the LCV reduced the blood pressure and heart rate in rats (12). As the properties of this factor were similar to those of FAD, we examined whether FAD functions as an stimulator of neuronal NOS acting by some other mechanism than as a coenzyme for NOS.

MATERIALS AND METHODS

Preparation of NOS. Neuronal NOS was purified by a reported method (13) with minor modifications. Briefly, whole rat brains were homogenized in buffer A (25 mM Tris-HCl, 0.5 mM EDTA, 1 mM dithiothreitol and 10 mg/ml leupeptin, pH 7.4) and centrifuged at 30,000 x *g* for 30 min. The supernatant was purified by 2',5'-ADP agarose affinity chromatography and eluted with 10 mM NADPH in buffer A. The eluate was applied to an FPLC MonoQ anion exchange column and eluted with a gradient of 0 - 0.4 M NaCl in buffer A.

Enzyme assay. NOS activity was determined by measuring the formation of citrulline. The complete reaction mixture (300 µl) contained a partially purified preparation of NOS (15 µg), 50 mM Tris-HCl (pH 7.4), 1 mM NADPH, 1.3 mM L-arginine, calmodulin (6 µg/ml), 1.6 mM $CaCl_2$, 50 µM (6R)-5,6,7,8-tetrahydrobiopterin and various amounts of flavins. The mixture was incubated for 5 min at 37 °C and then boiled for 30 sec at 100 °C to stop the reaction. Citrulline in the reaction mixture was determined by the method of Schmidt et al. (14).

Preparation of NOS activating factor. Bovine adrenals were boiled in 0.1 N HCl for 20 min and homogenized in a Polytron homogenizer. The homogenate was centrifuged at 7,000 x *g* for 30 min and the supernatant was subjected to ultrafiltration using a Centricut (U-10, Kurabou Co., Osaka). The ultrafiltrate was applied to a Sep-pak plus (C_{18}) (Millipore, Bedford) equilibrated with 0.1% trifluoroacetic acid (TFA). The column was washed with 20 ml of 0.1% TFA and developed with 50% acetonitrile containing 0.1% TFA. The eluate containing the factor was lyophilized, dissolved in buffer B (25 mM Tris-HCl, pH 9.0), and applied to an FPLC MonoQ anion exchange column HR 5/5 (Pharmacia, Uppsala) equilibrated with buffer B, and the column was developed with a gradient of 0 - 0.4 M NaCl in buffer B.

Phosphodiesterase treatments of NOS activating factor and FAD. NOS activating factor partially purified from bovine adrenals and FAD were treated with 1 unit / ml phosphodiesterase I (Type II, from Crotalus adamanteus venom, Sigma, St. Louis) for 12 h

The material on this page was copied from the collection of the National Library of Medicine by a third party and may be protected by U.S. Copyright law.

noncovalently

NOS (12). Its
(12). As the
FAD functions
coenzyme for

13) with minor
mM Tris-HCl,
centrifuged at
garose affinity
is applied to an
NaCl in buffer

on of citrulline.
ration of NOS
e, calmodulin
arious amounts
d for 30 sec at
l by the method

1 N HCl for 20
centrifuged at
ing a Centricut
ak plus (C_{18})
he column was
ing 0.1% TFA.
mM Tris-HCl,
5 (Pharmacia,
gradient of 0 -

ctivating factor
th 1 unit / ml
Louis) for 12 h

The material on this page was copied from the collection of the National Library of Medicine by a third party and may be protected by U.S. Copyright law.

at 37 °C in 20 mM Tris-HCl (pH 7.4) containing 5 mM $MgCl_2$. The reaction was stopped by adding 10 µl of 0.2 N HCl and boiling for 5 min. Samples were lyophilized and dissolved in 200 µl of 25 mM Tris-HCl (pH 7.4). Then their effects on NOS activity were determined.

Measurement of blood pressure. Male Wistar strain rats, weighing 200-300 g, were anesthetized (urethane, 1g/kg, *ip*). Then an intracranial catheter of polyethylene tubing (PE-10, Clay Adams, NJ) was inserted into the LCV, and another catheter made of polyethylene tubing (PE-50) was inserted into the left femoral artery for measurement of the blood pressure. FAD or artificial cerebrospinal fluid (aCSF) was injected into the LCV and the arterial blood pressure was recorded through the arterial catheter with an amplifier (Star Seimitsu Co., Tokyo) equipped with a transducer.

RESULTS AND DISCUSSION

The elution profiles of the NOS activating factor was determined using a preparation of NOS from rat brain partially purified by 2',5'-ADP agarose affinity chromatography and MonoQ column chromatography. NOS activity was determined by measuring the formation of either citrulline or nitrite and nitrate. Nitrite and nitrate were determined by the methods of Bredt and Snyder (15) and Pollock *et al.* (16). Both assays gave similar results. NOS activating factor was partially purified from bovine adrenals using Sep-pak (C18) and MonoQ column chromatography. As shown in Fig. 1, the elution profile of NOS activating factor was similar to that of FAD. Furthermore, the fraction containing NOS activating factor was yellow like FAD solution. Next, we studied the effect of FAD on neuronal NOS. As shown in Fig. 2A, exogenous FAD activated neuronal NOS dose-dependently, its effect being maximal at 10 µM and decreasing at higher concentrations. Figure 2B shows the elution profiles of NOS from a MonoQ column assayed in the presence and absence of 10 µM FAD. As shown in this figure, only one peak of NOS activity was recovered, and this peak activity was elevated by FAD. Since FAD has a phosphodiester bond, we examined the effect of phosphodiesterase on the ability of FAD to stimulate NOS. As expected, treatment of FAD with phosphodiesterase (1 U / ml for 12 h at 37 °C) completely abolished its stimulatory activity on NOS (Fig. 3). This treatment also abolished the stimulatory activity of the NOS activating factor extracted from bovine adrenals (Fig. 3). In contrast, pronase E treatment did not reduce the stimulatory activity of the NOS activating

04/25/2002 11:04 3016567246 TOP SHELF INC PAGE 08

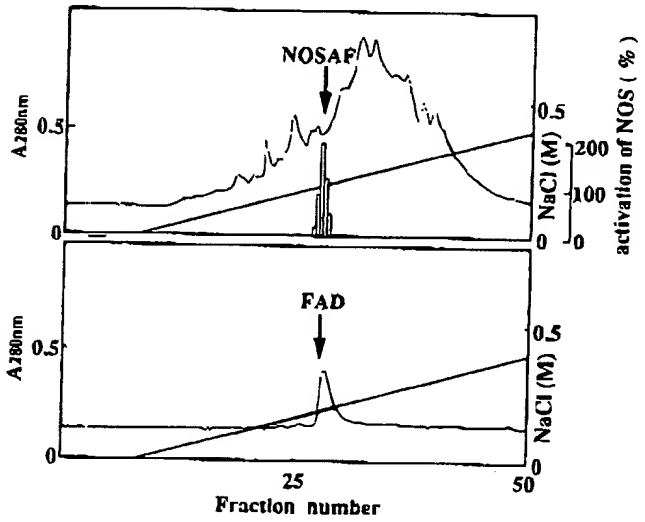

Fig. 1

Elution patterns of NOS activating factor and FAD on MonoQ column chromatography.

Samples of NOS activating factor and FAD (50 µmol) were applied to a MonoQ column and eluted with a linear gradient of NaCl. The effect of each fraction on NOS activity was determined.

factor (data not shown). Diadenosinetriphosphate (AP_3A) and diadenosinetetraphosphate (AP_4A) are known to be vasodilators with phosphodiester bonds (17). However, neither of them directly affected the brain NOS activity (data not shown). From these facts, it seems likely that the NOS activating factor is an FAD-related compound.

NOS is known to contain FAD which binds to the enzyme tightly by noncovalent interaction. However, some of the FAD might be dissociated from NOS during its purification, and this may be why the purified NOS preparation was activated by exogenously added FAD. To examine this possibility, NOS preparation was incubated with 50 µM FAD, which was 5-fold higher than the concentration required for full activation, and then separated NOS from free FAD rapidly on a small gel filtration column (Sephadex G-50, Pharmacia, Uppsala)(Fig. 4). NOS activity was recovered in fractions 8-10 and FAD in fractions 18-27. The recovered enzyme was stimulated 2-fold by exogenously added FAD. This result indicates that the mechanism by which exogenous FAD activates NOS is different from that of its function as a cofactor, that is, FAD further activates the holoenzyme. We examined the mode of NOS activation by FAD further by kinetic analyses.

The material on this page was copied from the collection of the National Library of Medicine by a third party and may be protected by U.S. Copyright law.

04/25/2002 11:04 3016567246 TOP SHELF INC PAGE 09

The material on this page was copied from the collection of the National Library of Medicine by a third party and may be protected by U.S. Copyright law.

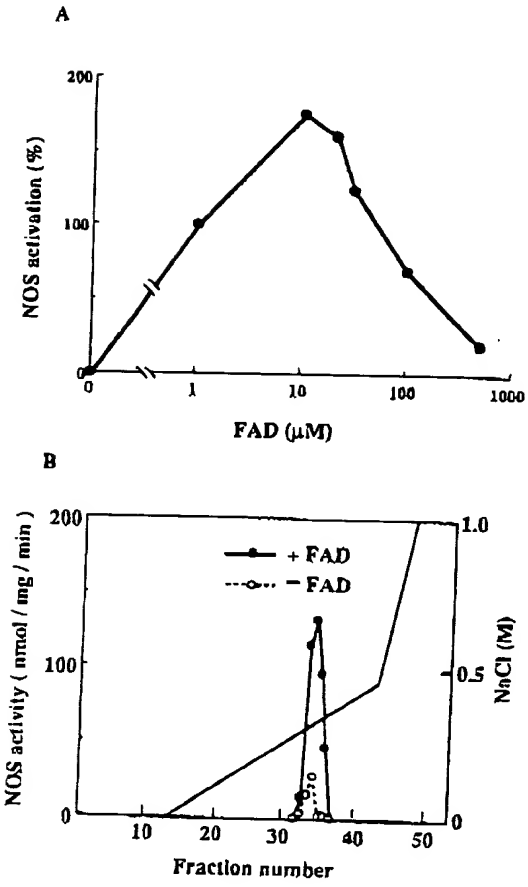

Fig. 2

Effect of FAD on NOS purified by MonoQ column chromatography.

(A) Dose-dependency of NOS activation by FAD. (B) Effect of FAD on NOS activity. NOS was purified from rat brain on 2',5'-ADP agarose and applied to a MonoQ column. The NOS activity of each fraction of eluate was measured in the presence (closed circles) or absence (open circles) of 10 μM FAD.

First, we examined the substrate (L-arginine) dependency of NOS in the presence and absence of FAD (10 μM). As shown in Fig. 5A, formation of the product (citrulline) during incubation (5 min at 37 °C) showed substrate dependency and saturation with and without added FAD. Lineweaver-Burk plots (Fig. 5B) were linear in the presence of FAD, indicating a Km value of about 20 μM. In the absence of FAD, however, these plots were not linear and indicated negative cooperativity in the reaction (Fig. 5B). Hill plots (Fig. 5C) gave a Hill coefficient of 0.75 in the absence of FAD, confirming the negative cooperativity. On the other hand, the Hill coefficient was 1.0 in the presence of FAD,

04/25/2002 11:04 3016567246 TOP SHELF INC PAGE 10

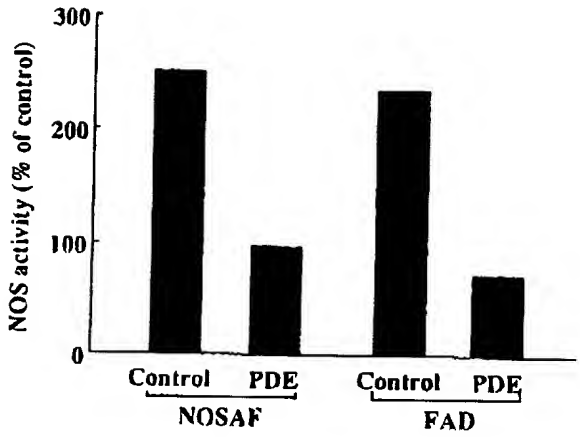

Fig. 3

Effects of phosphodiesterase treatment on the activities of NOS activating factor and FAD.

The NOS activating activities of samples of NOS activating factor partially purified from bovine adrenals and 10 nmol of FAD with and without treatment with phosphodiesterase (1 U / ml) for 12 h at 37°C were measured.

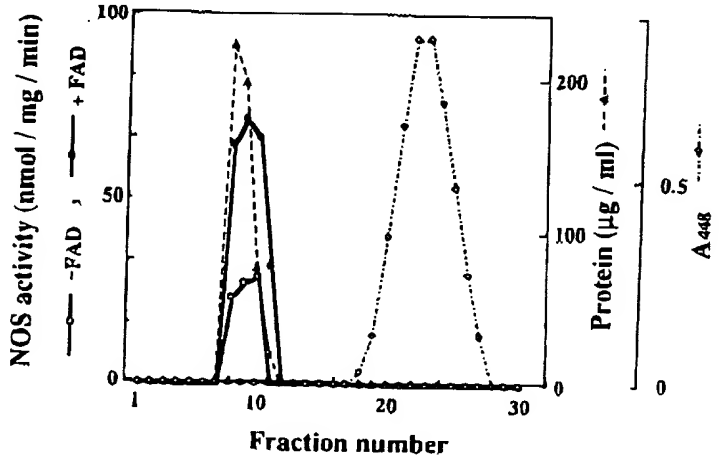

Fig. 4

Effect of pretreatment of NOS with FAD.

NOS was treated with 50 μM FAD for 1 h at 4 °C. Then, NOS was separated from FAD on a Sephadex-G-50 column equilibrated with buffer A and the NOS activities of fractions of eluate from Sephadex G-50 were measured in the presence (closed circles) or absent (open circles) of 10 μM FAD.

The material on this page was copied from the collection of the National Library of Medicine by a third party and may be protected by U.S. Copyright law.

04/25/2002 11:04 3016567246 TOP SHELF INC PAGE 11

The material on this page was copied from the collection of the National Library of Medicine by a third party and may be protected by U.S. Copyright law.

r and FAD.
' purified from
odiesterase (1

A 448

ted from FAD
of fractions of
absent (open

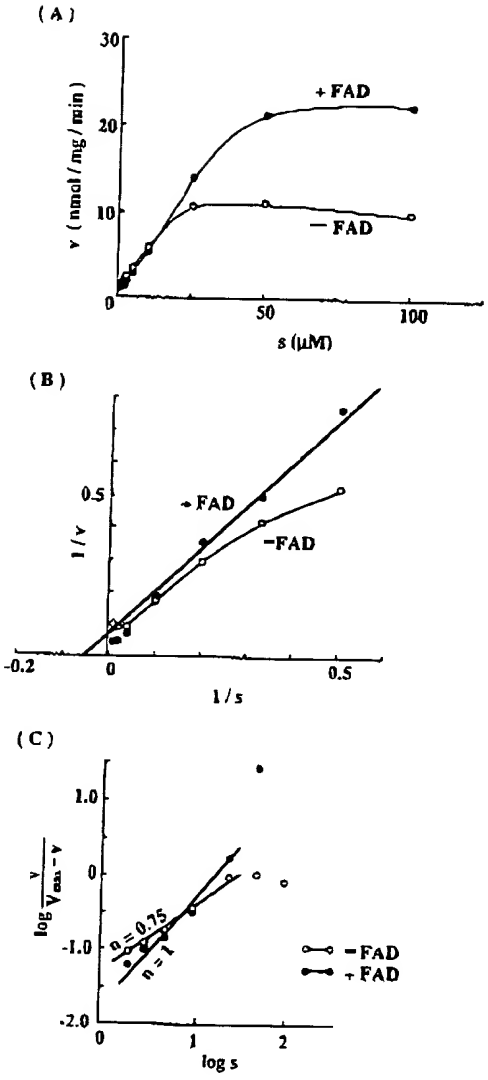

Fig. 5

Kinetic analyses.

NOS was assayed with various concentrations of *L*-arginine in the presence (closed circles) or absence (open circles) of 10 μM FAD. (A) Substrate dependency, (B) Lineweaver-Burk plots, (C) Hill plots. "n" represents the slopes of the lines, Hill coefficients.

04/25/2002 11:04 3016567246 TOP SHELF INC PAGE 12

indicating the absence of cooperativity in this reaction. Thus, kinetic analyses showed that in the absence of FAD, NOS exhibited negative cooperativity in the enzyme reaction due to substrate binding to NOS and that negative cooperativity was completely suppressed by FAD, judging from the Hill coefficient of 1.0. This effect might explain the mechanism of NOS activation by exogenous FAD. Cooperativity of substrate binding is usually observed in oligomeric enzymes with multiple substrate binding sites. Probably NOS is an oligomer in the absence of FAD and the interaction between each subunit is affected by FAD. Several studies have indicated that neuronal NOS is a dimer (18,19.20), but others have indicated that it is a monomer (4,21). Those findings and the present results suggest that the dimeric form of NOS might be inactive, and the dimer might be dissociated by a NOS activator such as FAD to an active form. To substantiate this hypothesis, it will be necessary to determine the molecular weights of NOS in the absence and presence of FAD.

We have found that injection of NOS activating factor partially purified from bovine adrenals into the LCV of rats resulted in decrease in their blood pressure and heart rate (12). To determine whether FAD has similar effects, we injected it into the LCV of rats under anesthesia with urethane. As shown in Fig. 6, FAD injection lowered the blood pressure. Decrease in the heart rate was also observed after LCV injection of FAD (data not shown). This hypotensive effect was not observed when N^G-monomethyl-*L*-arginine, an NOS

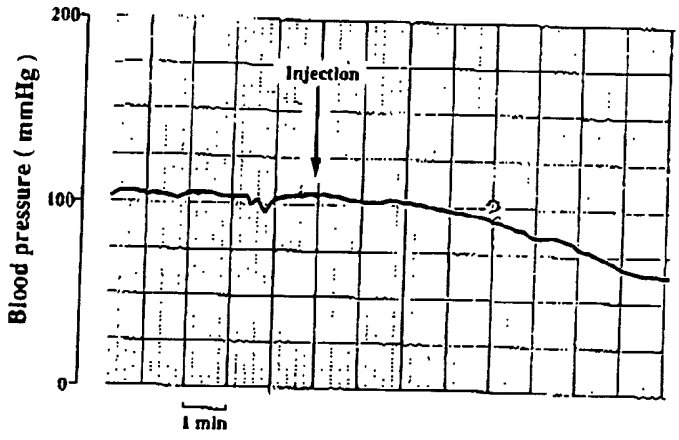

Fig. 6

Effect of FAD injection into the lateral cerebral ventricle on the blood pressure.

FAD (10 µl of 5 mM solution in artificial CSF) was injected into the LCV of a rat anesthetized with urethane and the blood pressure was monitored.

The material on this page was copied from the collection of the National Library of Medicine by a third party and may be protected by U.S. Copyright law.

04/25/2002 11:04 3016567246 TOP SHELF INC PAGE 13

The material on this page was copied from the collection of the National Library of Medicine by a third party and may be protected by U.S. Copyright law.

inhibitor, was injected into the LCV before FAD (data not shown). These findings suggest that the decreases in the blood pressure and heart rate induced by FAD were elicited through activation of NOS in the brain. However, this raises the problem of whether the effect of FAD on NOS is caused by direct activation of the enzyme or by an indirect effect such as activation of some receptor for FAD on the surface membrane of cells. This problem requires investigation.

In rats, the concentrations of FAD in the serum and brain cells are about 25 nM and 3.5 μM, respectively, and that of *L*-arginine in the serum is about 100 μM, although its intracelluar concentration is not yet known. Supposing that a concentration of about 100 μM *L*-arginine usually elicits negative cooperativity in the reaction catalyzed by brain NOS and that FAD eliminates this negative cooperativity intracellularly, it can be supposed that *L*-arginine at concentrations of below 100 μM shows negative cooperativity on NOS activity in neuronal cells by converting the enzyme to a dimer and that exogenous FAD eliminates its effect by converting the enzyme to a monomer state. Alternatively, FAD may stimulate NOS through some receptor on the cell surface.

ACKNOWLEDGEMENTS

This work was partly supported by a Grant-in-Aid of Scientific Research No. 01570133 from the Ministry of Education, Science and Culture of Japan.

REFERENCES

1. Furchgott, R.F. (1990) Acta Physiol. Scand., 139, 257-270.
2. Moncada, S., Palmer, R.M.J., and Higgs, E. A. (1991) Pharmacol. Rev., 43, 109-142.
3. Snyder, S. H., and Bredt, D.S. (1992) Sci. Am., 266, 68-77.
4. Bredt, D.S., and Snyder, S.H. (1990) Proc. Natl. Acad. Sci. USA, 87, 682-685.
5. Lamas, S., Marsden, P.A., Li, G.K., Tempst, P., and Michel, T. (1992) Proc. Natl. Acad. Sci. USA, 89, 6348-6352.
6. Yui, Y., Hattori, R., Kasuga, K., Eizawa, H., Hiki, K., and Kawai, C. (1990) J. Biol. Chem., 266, 12544-12547.
7. Iida, S., Ohshima, H., Oguchi, S., Hata, T., Suzuki, H., Kawasaki, H., and Esumi, H. (1992) J. Biol. Chem., 267, 25385-25388.
8. Nunokawa, Y., Ishida, N., and Tanaka, S. (1993) Biochem. Biophys. Res. Commun., 191, 89-94.

04/25/2002 11:04 3016567246 TOP SHELF INC PAGE 14

9. Bredt, D.S., Hwang, P.M., Glatt, C.E., Lowenstein, C., Reed, R.R., and Snyder, S.H. (1991) Nature, 351, 714-718.
10. Mayer, B., John, M., Heinzel, B., Werner, E.R., Wachter, H., Schultz, G., and Böhme, E. (1991) FEBS Lett., 288, 187-191.
11. Bredt, D.S., Ferris, C.D., and Snyder, S.H. (1992) J. Biol. Chem., 267, 10976-10981.
12. Hashida-Okumura, A., Nagai, K., and Nakagawa, H. (1994) J. Clin. Biochem. Nutr., in press.
13. Hope, B.T., Michael, G. J., Knigge, K.M., and Vincent, S.R. (1991) Proc. Natl. Acad. Sci. USA, 88, 2811-2814.
14. Schmidt, H.H.H.W., Wilde, P., Evers, B., and Böhme, E. (1989) Biochem. Biophys. Res. Commun., 165, 284-291.
15. Bredt, D.S., and Snyder, S.H. (1989) Proc. Natl. Acad. Sci. USA, 88, 2811-2814.
16. Pollock, J.S., Förstermann, U., Mitchell, J.A., Warner, J.D., Schmidt, H.H.H.W., Banade, M., and Murad, F. (1991) Proc. Natl. Acad. Sci. USA, 88, 10480-10484.
17. Pohl, U., Ogilvie, A., Lamontagne, D., and Busse, R. (1991) Am. J. Physiol., 260, H 1692-H 1697.
18. Schmidt, H.H.H.W., and Murad, F. (1991) Biochem. Biophys. Res. Commun., 181, 1372-1377.
19. White, K.A., and Marletta, M.A. (1992) Biochemistry, 31, 6627-6631.
20. Schmidt, H.H.H.W., Pollock, J.S., Nakane, M., Gorsky, L.D., Förstermann, U., and Murad, F. (1991) Proc. Natl. Acad. Sci. USA, 88, 365-369.
21. Mayer, B., John, M.,and Böhme, E. (1990) FEBS Lett., 277, 215-219.

The material on this page was copied from the collection of the National Library of Medicine by a third party and may be protected by U.S. Copyright law.